CRANFIELD UNIVERSITY

M. H. THOMAS

FOULING CHARACTERISTICS OF MEMBRANE FILTRATION APPLIED TO WASTEWATER

SCHOOL OF WATER SCIENCES

MSc THESIS

CRANFIELD UNIVERSITY

SCHOOL OF WATER SCIENCES

MSc THESIS

Academic Year 1997-8

M. H. THOMAS

Fouling characteristics of membrane filtration applied to wastewater

Supervisor: S. J. Judd

September 1998

This thesis is submitted in partial fulfilment of the requirements
for the degree of Master of Science

ABSTRACT

The use of microfiltration and ultrafiltration in waste water treatment is attracting increasing interest. The problem of membrane fouling and the high costs associated with the process has limited large scale applications. This study forms part of a project to optimise the design of a membrane bioreactor.

A pilot plant has been used to assess the performance of three tubular membrane modules. The wastewater used has been taken from an existing biological reactor to simulate the conditions found in a membrane bioreactor. Commercially available membrane modules of different specification have been tested. The study has centred around the fouling characteristics of the membranes under varying operating conditions.

The flux produced after 24 hours continuous operation has been used to assess the degree of fouling present. The hydrodynamic conditions have been varied, and an optimal cross flow velocity range has been identified.

The feed wastewater has been varied, and the specific flux at different MLSS concentrations recorded. The specific flux shows a decline with increasing MLSS concentration. The magnitude and rate of this decline is membrane dependant.

The permeate product water shows a reduction of more than 99% for SS, BOD_5 and COD over the feed stream under all conditions used. The DOC also shows a reduction of up to 72%, indicating that the membranes reject a portion of the high molecular weight molecules present in the feed stream.

The energy consumption has been estimated from the final permeate flux produced under each set of conditions. The lowest value has been found to be 1.75 $kWhm^{-3}$, which was achieved at the lowest cross flow velocity used during the trials. This illustrates the influence of pressure drop through the system, which is proportional to the flow velocity squared.

ACKNOWLEDGEMENTS

I would like to thank the project sponsor, Anglian Water Services Ltd, and in particular my project supervisor, John Gibson, for his invaluable help and advice. I would also like to thank staff within the membrane group of Anglian Water Innovation, and all at the Innovation centre in Cambridge.

I would also like to thank my academic supervisor, Dr Simon Judd, for his help and guidance. The advice of other members of the School of Water Sciences, Cranfield University, is gratefully acknowledged.

EXECUTIVE SUMMARY

I. INTRODUCTION

The use of biological processes for the treatment of wastewater is well established. These processes occur in two stages: the biochemical reactions, followed by a solid-liquid separation step. After separation, the clarified effluent is discharged and the solids returned to the reactor or wasted from the system. The use of membrane filtration for the solid-liquid separation step is known as a membrane bioreactor (MBR).

A joint project has been undertaken to optimise the design of an MBR. The biological process optimisation is being carried out at Lund University, Sweden. The membrane filtration performance is being investigated by Purac, UK. This thesis details experiments performed to assess the filtration behaviour of commercially available membranes, under a range of operating conditions.

II. BACKGROUND WORK

A. Overview of MBRs

Research into MBR development is widespread, and results from pilot and full scale plants show a number of advantages:

- Small foot print
- High quality effluent
- Improved control over biochemical reactions
- Reduced sludge production

There are two generic configurations for an MBR, integrated and side-stream:

An integrated MBR has membrane modules submerged within the reactor. The permeate is forced through the membrane by the static hydraulic head in the reactor or by creating a negative pressure on the permeate side with a suction pump.

A side-stream MBR has the membrane modules outside the reactor. The mixed liquor must be pumped through the modules and the retained sludge returned to the reactor. In this case the driving pressure is provided by the recirculation pumps.

The membranes used in an MBR are usually microfiltration or ultrafiltration type, and those in a side-stream MBR are operated in the cross flow configuration. This study has been based on tubular membranes suitable for a side-stream MBR.

B. Membrane fouling

Fouling is a general term for the build up of particles and solutes on, or within, the membrane. Membrane filtration is a pressure driven process, and the passage of water through the membrane carries fouling material to the surface. The membrane is a size selective barrier, therefore matter which is rejected will concentrate at the membrane surface.

The species which accumulate at the membrane surface will reduce the hydraulic permeability. The type of fouling occurring depends on the nature of the filtered solution:

- Concentration polarisation - a high concentration of dissolved molecules
- Gel layer - solutes which exceed their solubility constant due to polarisation precipitate at the membrane surface
- Cake layer - particulate matter transported to the surface and deposited

The degree of fouling which occurs depends on three factors:

- Membrane type

The design and geometry of the membrane module will affect the flow characteristics through it. The membrane material can affect adsorption onto the surface. The porosity will affect the degree of concentration polarisation as well as the permeate flux.

- Operating conditions

The convection to and diffusion away from the membrane surface affects the rate and extent of fouling. The driving pressure has a direct effect on the permeate flux produced, and hence the rate of transport to the surface.

- Solution characteristics

Factors such as solids concentration, pH and particle size can have a strong influence on the surface fouling. The micro-organisms present in biological solutions can also affect the degree of fouling.

C. Fouling control

During filtration of solutions and suspensions a build up of fouling will cause a decline in the permeate flux. When the flux declines below a certain level it will become uneconomical to continue the process. Techniques used to remove fouling deposits and/or reduce the rate of build up include:

- Chemical or physical membrane cleaning
- Solution modification
- Hydrodynamic modification
- Sub-critical flux operation

III. AIMS AND OBJECTIVES

The principle objectives of this study have been to investigate the fouling characteristics of three membrane modules under a range of operating conditions. These modules are of the same geometry, and are therefore directly comparable. The membranes are compared for:

- Four feed solution concentrations
- Three cross flow velocities

The optimum set of operating conditions will be determined in terms of permeate flux per unit pressure, and the most economical hydrodynamic conditions in terms of energy consumption per unit permeate produced.

The feed solution and permeate are analysed for key contaminants, and the rejection of each membrane assessed.

Some methods of fouling reduction involving specific hydrodynamic conditions are also investigated

IV. EXPERIMENTAL

The experimental work has been performed on a purpose built filtration test rig. The rig is located at the Anglian Waste Water Innovation Centre, Cambridge. Feed sludge is drawn from an existing biological reactor into a $1m^3$ feed reservoir on the rig. The sludge can be concentrated up to the desired concentration in this reservoir.

The rig consists of two parallel streams, each of which can accommodate one membrane module of up to 3m in length. Once initiated, the rig runs under PLC control until it is stopped manually or by a safety cut out. Instruments monitor the feed and permeate flow rates and the trans-membrane pressure, and a data logger records the data streams.

Analysis of samples taken from the feed reservoir and both permeate streams are analysed by Anglian Water laboratories (Whitlingham) for the following contaminants: TSS, BOD_5, COD, NH_3-N, TKN and DOC. The temperature of the sludge is monitored during runs, as is the turbidity of the permeate streams.

V. RESULTS

A. Clean water flux

With the feed reservoir filled with tap water, the flux produced by each membrane was determined for increasing trans-membrane pressure. The results show that flux increases

in direct proportion to increasing pressure at $\Delta P < 1$ bar. Further increases in pressure yield lower increases in flux.

B. Flux decline due to fouling

Continuous filtration of wastewater for 24 hours gives a good indication of fouling behaviour. Initial fouling occurs and the flux drops rapidly in the first minutes. The flux decline over the remaining hours shows that a gradual increase in fouling is occurring.

C. Final specific flux

The flux per unit pressure (specific flux) after 24 hours has been used to compare the degree of fouling present for each set of conditions used. The final specific flux has been measured for each membrane at TSS concentrations of 2,500, 5,000 and 7,500 mgl^{-1} and cross flow velocities of 2.3, 3.1 and 3.9 ms^{-1}.

In almost all cases, the highest value for the final specific flux occurs at 3.1 ms^{-1}. Using this optimum cross flow velocity, the membranes have been compared at TSS concentrations of 2,500, 5,000, 7,500 and 15,000 mgl^{-1}. These results clearly show the differences in behaviour of the membrane modules tested.

D. Sample analysis

A comparison between the levels of contaminants in the feed sludge and those in the permeate gives a direct indication of the selectivity of each membrane.

Due to the low pore size of the membranes used, the removal of particulate matter was consistently high. The TSS measured was normally below the limit of detection.

E. Energy consumption

The energy required to supply the recirculating feed flow can be calculated from the feed flow rate and the pressure drop through the system. A useful measure of energy consumption is the energy required per unit permeate produced ($kWhm^{-3}$).

The energy consumption after 24 hours operation varied with the changing conditions used during the trials. The values ranged between 1.75 and 50.6 $kWhm^{-3}$.

F. High flow rate flushes

Preliminary trials have been performed to test a novel fouling reduction technique. The aim was to periodically increase membrane surface scour, while simultaneously removing convective transport to the membrane surface. The results show a small reduction in flux decline.

G. Investigation into sub-critical flux operation

Preliminary trials were performed at a low ΔP in an attempt to operate in the sub-critical pressure region. Although a stable flux was maintained, ΔP increased gradually throughout the runs. This indicates that fouling was occurring and a dynamic balance was not reached.

VI. DISCUSSION

A. Clean water flux

The results from the clean water flux vs. pressure trials have been used to calculate the resistance of the membrane in the absence of fouling. These values show that there is a significant difference between the modules in the resistance to clean water. This indicates a difference in porosity. Similar results have been obtained by Magara and Itoh (1991).

B. Filtration of wastewater

The specific flux produced by each membrane under different cross flow velocities and SS concentrations shows some clear trends. The maximum specific flux is achieved at a cross flow velocity of 3.1 ms^{-1} under most conditions. This is probably because at higher velocities the increased trans-membrane pressure exceeds the critical pressure. Above this value, the flux does not increase in proportion to increasing pressure. This agrees with the results reported by Howell (1996).

The direct comparison between membrane modules shows that membrane performance can vary dramatically. As the modules are of the same geometry, these differences are likely to be due to differences in porosity and membrane material.

C. Product water quality

The removal of particulate matter was greater than 99% for all membranes tested. This result is in good agreement with previously published results. Through almost complete removal of particulate matter, levels of other contaminants are also reduced. The permeate showed over 99% reduction in BOD_5 and COD. Levels of DOC also showed a reduction, indicating the membranes are rejecting a portion of the high molecular weight molecules in solution.

These levels of contaminant rejection are in agreement with previously reported results using membranes of similar pore size (Trouve *et al.*, 1994, Cicek *et al.*, 1998). There is no significant difference in the rejection characteristics of the three membranes tested.

D. Energy consumption

The energy consumption for filtration shows a wide range of values. This is due to the differences in performance of the membranes with changing conditions. The lowest value of energy consumption occurs using the lowest cross flow velocity. This is due to the effect of velocity on pressure losses through the system - frictional losses are proportional to velocity squared.

E. Headloss due to friction

The losses calculated through the system are high, and form a large part of the measured trans-membrane pressure. Much of the pressure provided by the pumps is lost due to friction and the pressure available to drive filtration is lower than that recorded by the gauges.

F. Hydrodynamic variations to reduce fouling

The trials were performed at low driving pressure were aimed at operating below the critical pressure. However, as the trans-membrane pressure increased steadily during the run, fouling was gradually increasing. Previous studies reporting successful sub-critical flux operation have utilised turbulence enhancing devices. It is likely that a the low flow rates used in this trial, the membrane wall shear was not high enough to sustain a dynamic balance.

The use of periodic high flow rate flushes through the membrane module has been tested for a reduction in fouling build up. Lack of experimental time allowed only preliminary investigations to be completed. The results are inconclusive as experimental error could account for the differences seen.

VII. CONCLUSIONS

There can be significant differences in the performance of membranes with a similar specification.

The permeate flux has a strong dependence on SS concentration and velocity of the feed stream. In these trials, the optimum velocity in terms of specific flux production is approximately $3ms^{-1}$.

The permeate product water contains negligible levels of SS and BOD_5. The permeate quality is similar for all membranes tested.

Energy consumption showed a minimum of 1.75 $kWhm^{-3}$ at a cross flow velocity of 2.3 ms^{-1}. This illustrates that increased cross flow velocity generates higher frictional losses, and increases operating costs.

VIII. SUGGESTIONS FOR FURTHER WORK

Two of the membrane modules used in these trials (M1 and M2) have a very similar specification. Their performance under the same conditions shows large differences. The reasons for this must lie with the material and/or pore structure. A thorough investigation of the surface properties of the two materials is recommended.

Sub-critical flux operation offers attractive benefits (removal of the need to clean the membranes), and further investigations are recommended.

The high flow rate flushing technique requires a structured experimental investigation to determine the efficacy and economic viability.

CONTENTS

FIGURES

TABLES

NOTATION

Symbol	Meaning	Units
J	Permeate flux	$lm^{-2}h^{-1}$ or $m^3m^{-2}s^{-1}$
J_{abs}	Absolute flux	$lm^{-2}h^{-1}bar^{-1}$
J_T	Permeate flux at temperature T	$lm^{-2}h^{-1}$ or $m^3m^{-2}s^{-1}$
ΔP	Pressure difference	bar, Nm^{-2} or Pa
ΔP_C	Critical trans-membrane pressure difference	bar, Nm^{-2} or Pa
TMP	Trans-membrane pressure	bar, Nm^{-2} or Pa
$\Delta\pi$	Osmotic pressure difference	bar, Nm^{-2} or Pa
ρ	Density	Kgm^{-3}
υ	Cross flow velocity	ms^{-1}
μ	Viscosity	Nsm^{-2}
R_m	Hydraulic resistance of a membrane	m^{-1}
R_{CP}	Resistance of concentration polarisation layer	m^{-1}
R_G	Resistance of gel layer	m^{-1}
R_C	Resistance of cake layer	m^{-1}
R_F	Combined resistance due to all fouling	m^{-1}
C_B	Concentration of bulk solution	$molm^{-3}$
C_M	Concentration at membrane surface	$molm^{-3}$
C_P	Concentration of permeate	$molm^{-3}$
δ	Boundary layer thickness	m
D	Diffusion coefficient	m^2s^{-1}
k	Mass transfer coefficient	ms^{-1}
Re	Reynolds number	-
Sc	Schmidt number	-
Sh	Sherwood number	-
d	Characteristic hydraulic dimension of system	m
f	Friction factor	-
L	Length of pipe	m
h	Headloss	m of water or bar

Acronym	Meaning	Units
RAS	Settled sludge returned to reactor	-
SS	Suspended Solids	mgl^{-1}
MLSS	Mixed Liquor Suspended Solids. The SS present in liquor from a biological reactor	mgl^{-1}
BOD_5	Biological Oxygen Demand over 5 days	mgl^{-1}
COD	Chemical Oxygen Demand	mgl^{-1}
TKN	Total Kjeldahl Nitrogen	mgl^{-1}
DOC	Dissolved Organic Carbon	mgl^{-1}
NH_3-N	Ammoniacal Nitrogen	mgl^{-1}
MWCO	Molecular Weight Cut Off	Da

1. INTRODUCTION

The use of biological processes for the treatment of domestic, municipal and some industrial wastewaters is well established. These processes occur in two stages: the biochemical reactions, followed by a physical separation step. The biomass and solids removed during separation are either returned to the reactor or removed from the system.

The combination of membrane filtration with biological reactors for the treatment of wastewater is attracting increasing interest. Membrane filtration can be used in place of traditional methods of biomass retention and effluent clarification, e.g. sedimentation. This process combination is known as a membrane bio-reactor (MBR). The use of a membrane for solid-liquid separation has a number of advantages including: small footprint, high quality product water (permeate) and better biological performance due to tighter control over biological conditions.

The small footprint of an MBR can be important where there is a shortage of land or costs are high. The quality of the permeate can be controlled through membrane selection and tailored to the discharge consent granted. The improved control over the biological performance can improve the treatment of high strength wastewater and lead to lower sludge production, reducing sludge handling and disposal costs.

The major limitations of using membrane processes for this application are economic. The capital cost of membranes is high and their useful life short compared to conventional separation techniques. The driving force for membrane separation processes is pressure, hence operating costs are also high. For MBRs to be economically viable, the membrane separation step must be designed for optimum efficiency.

A joint project between Purac Ltd, UK and Lund University in Sweden has been undertaken to optimise the design of an MBR. The biological process optimisation is being carried out at Lund University. The membrane filtration performance is being investigated by Purac. A membrane pilot plant has been constructed for this purpose. By operating the pilot plant under different conditions, an optimum operating regime can be determined for the desired biological conditions.

During the filtration of biomass, there is a tendency for solids to be deposited on the surface of the membrane. The deposition of particles and solutes on and within the membrane structure is known as fouling. Understanding the causes and effects of fouling under different conditions is crucial to the optimisation of membrane filtration.

Membrane fouling causes a decline in permeate flux over time. This flux decline means that the permeate produced per unit energy is reduced. Traditional methods of fouling removal include physical and chemical cleaning. The provision of facilities to accommodate these techniques add to the cost and complexity of the membrane filtration plant.

Several investigations have revealed other methods of fouling control. These methods include changes to the solution, the membrane and the operating conditions.

In an MBR, solution characteristics are controlled to optimise the biological performance of a reactor. Hence, modification of the solution to improve the filtration performance may have a deleterious effect on the biological performance of the reactor. As the optimum conditions for biological treatment have yet to be reported by Lund University, the effect of different solution concentrations has been investigated.

Laboratory scale studies have shown that filtration performance can be improved by modification to the membrane module and the membrane surface. The pilot plant has been designed to test membrane modules which are commercially available. For these investigations, 'off the shelf' membrane modules have been tested and no chemical or physical changes have been made. However, differences in performance between the membranes used gives useful indications as to which parameters have a strong effect on flux and fouling.

The experiments conducted have centred around the effect of changes in operating conditions on the permeate flux produced and the degree of fouling occurring. The key parameters investigated are: Driving pressure, cross flow velocity and MLSS. The selectivity of the membranes has been assessed in terms of the rejection of key contaminants within the feed stream.

Many hydrodynamic methods of fouling reduction have been reported in published literature. Two modes of operation involving specific hydrodynamic conditions have been tested and their effect on fouling behaviour assessed.

A useful measure of the operating costs of running a membrane filtration is the energy consumption in terms of power used per unit permeate produced ($kWhm^{-3}$). The power required is determined by the hydrodynamic regime used. The energy consumption has been estimated for each mode of operation, and the most economical mode of operation has been identified.

2. LITERATURE REVIEW

2.1. Membrane Bioreactors: an overview

The combination of membrane filtration with a biological reactor for the treatment of wastewater is known as a membrane bioreactor (MBR). This technique was first reported by Smith *et al.* (1969). In this case an ultrafiltration membrane was used to separate activated sludge from the final effluent, with the biomass being recycled to the aeration tank.

In recent years, the application of membranes for solid/liquid separation in biological processes has increased. Membranes have been used in combination with aerobic (Sato and Ishii, 1991; Magara and Itoh, 1991; Ishiguro *et al.*, 1994) and anaerobic (Choo and Lee, 1996; Anderson *et al.*, 1986; Fakhru'l-Razi, 1994) treatment processes. Results of these studies have shown that the advantages of using membranes in this application include:

- Small footprint - membrane modules required to perform the separation have a smaller land area than the sedimentation tanks required to treat the same flow. The reactor can operate at a higher mixed liquor suspended solids (MLSS) concentration leading to a smaller volume needed to treat the same waste, hence a further reduction in overall footprint for the system.

- High quality effluent - the membranes used have a low pore size (typically 0.1 μm for microfiltration) which means the effluent suspended solids (SS) content is very low. The reduction in micro-organisms is much greater than for conventional techniques. When using an ultrafiltration membrane, Cicek *et al.* (1998) found that the effluent contained no heterotrophic micro-organisms and that the MS-2 virus was retained by the membrane.

- Better control over biological conditions - as the solid/liquid separation is complete, all sludge can be recycled to the reactor. This means that the sludge age is independent of hydraulic retention time, giving more control over the biological process. This can lead to reduced sludge production (Trouve *et al.*, 1994) and greater contaminant removal. The high shear environment found in some membrane configurations can lower the average particle size in the biomass (Bailey *et al.* 1994). This size reduction is thought to aid mass transfer in the biomass, giving a possible explanation to improved nutrient removal rates (AWWARF, LdE, WRC, 1996).

The biological reactor and membrane units of an MBR can be combined externally, where the biomass must circulate between the reactor and membrane (side-stream MBR) as shown in Figure 2.1a, or internally (integrated MBR), Figure 2.1b.

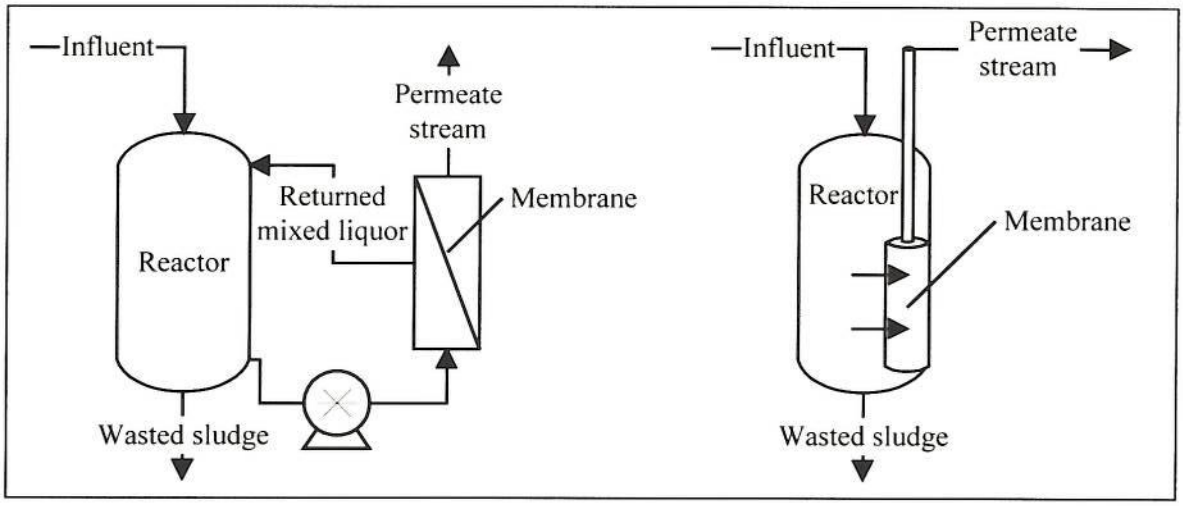

Figure 2.1a Side stream MBR **Figure 2.1b Integrated MBR**

Table 2.1 shows some examples of the performance of MBR systems, compared with typical performance of a biological reactor with conventional solid-liquid separation.

Optimising the design of the membrane separation process is complex due to a large number of depending factors. The majority of economic factors used during the design and control of membrane processes are based on the permeate flow recovered (Koltuniewicz and Noworyta 1994). In the following sections, the factors which affect membrane performance are outlined with reference to previous studies.

2.2. Membrane filtration used in MBRs

In both side-stream and integrated MBRs, either microfiltration (MF) or ultrafiltration (UF) membranes are used. These membranes have the selectivity to produce high quality permeate with a moderate driving pressure (0.1 - 10 bar) being applied. Generic details for MF and UF membranes are shown in Table 2.2 (Porter, 1986):

Table 2.2 MF and UF characteristics

Type	Pore size (μm)	Pressure drop (bar)
MF	0.05 - 10	0.1 - 2
UF	0.001 - 0.1	1 - 10

The Table above shows that there is some overlap between the two classes of filtration, the division normally being made by the manufacturer.

With an integrated MBR, the pressure to provide the driving force across the membrane must be either generated inside the reactor, or a vacuum applied to the permeate side of the membrane (Ueda *et al.*, 1996).

For the side-stream MBR, the pressure gradient across the membrane is normally provided by the recirculating flow (Muller *et al.*, 1995).

2.2.1. Side-stream MBR membranes:

The membranes used for side-stream MBRs are arranged in the cross-flow configuration, see Figure 2.2. This means that the biomass is pumped through the membrane module, permeate is recovered, and the retentate is returned to the reactor.

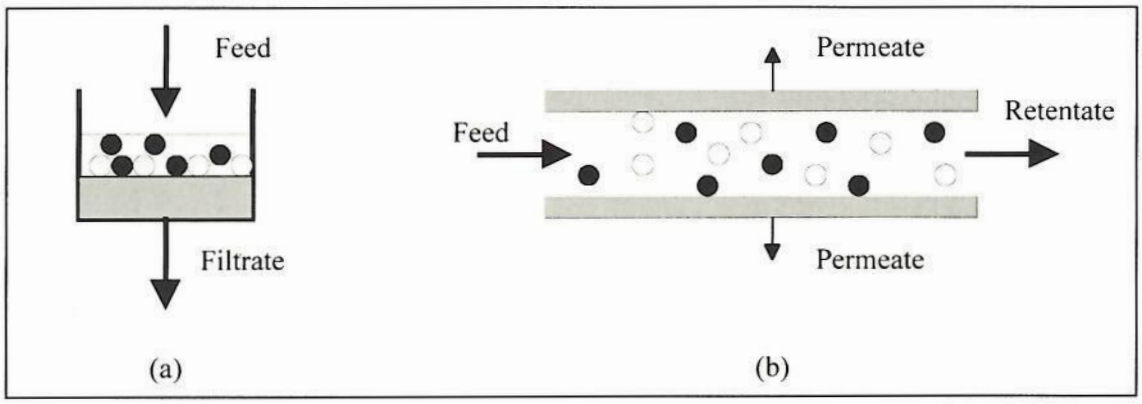

Figure 2.2 Schematic of (a) dead end and (b) cross-flow filtration

The performance of a membrane filtration system is described in terms of the flow of permeate per unit area per unit time - the permeate flux, J (in $m^3m^{-2}s^{-1}$ or $lm^{-2}h^{-1}$).

The permeate produced from membrane filtration has very low suspended solids (SS) concentration due to the low pore size (and hence high rejection) of the membranes. Several authors report complete SS removal, as shown in Table 2.3.

The permeate also has a low concentration of dissolved organic material, e.g. soluble COD. These high molecular weight molecules are not removed by conventional sedimentation. However, due to the low pore size of UF and the dynamic layer formed on MF some of these macromolecules are rejected. Table 2.3 shows typical removal rates of DOC for a selection of membranes:

Table 2.3 SS and DOC removal rates for membrane filtration

membrane type and pore size	SS removal %	DOC removal %	Reference
MF, 0.1 μm hollow fibre	100	25 - 33	Ueda *et al.* 1996
MF, 0.1μm ceramic hollow fibre	>99.9	63.5	Trouve *et al.* 1994
UF, 300 kDa ceramic tubular	>99.9	98.8	Cicek *et al.* 1998

During membrane filtration of biomass suspensions (as in the case of an MBR) there is a tendency for a fouling layer to build up on the surface of the membrane (Baker *et al.*, 1985; Porter, 1986; Fane and Fell, 1987; Howell, 1995; Suzuki, 1988). This fouling layer will increase the pressure required to produce a given flux, and the build up of this fouling layer must be accounted for during MBR design. DeFilippi and Goldsmith (1970) conclude that it is necessary to obtain pilot plant information on flux and retention for the particular application to determine the optimum process design.

2.3. What is membrane fouling?

Fouling is a general term given to the process by which a variety of species in the feed solution increase the membrane resistance. This increase in resistance may be due to particle deposits on the membrane surface, macromolecules adsorbing onto the surface or into the bulk membrane material, concentration polarisation or pore blocking. This increase in membrane resistance will exhibit itself as a decline in the permeate flux (Belfort and Altena, 1983).

To illustrate these phenomena, it is necessary to give a description of what is occurring at the surface of a membrane during cross flow filtration:

The feed solution flows over the surface of the membrane. There is a pressure difference between the retentate side and the permeate side, and this is the driving force which forces matter to pass through the membrane. The membrane is a size selective barrier to particles and solutes within the liquid. This can be represented as shown in Figure 2.3.

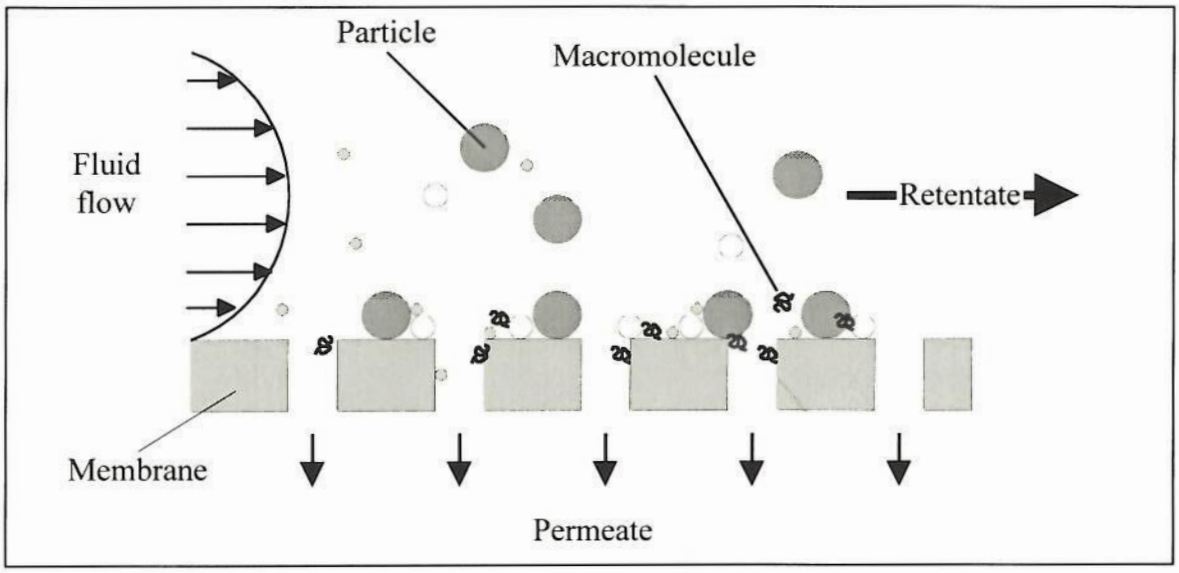

Figure 2.3 Diagram representing cross flow filtration with deposition and adsorption.

2.4. Pure water flux

The flux, J, of clean water across a membrane with no materials deposited on the surface can be described by Darcy's law (Al-Malack and Anderson, 1997), which relates the flux of liquid through a porous medium to the pressure drop across the medium:

$$J = \frac{\Delta P}{\mu . R_M} \qquad [2.1]$$

where J = permeate flux ($m^3m^{-2}s^{-1}$)
ΔP = pressure drop across the membrane (Nm^{-2})
μ = absolute viscosity of the water (Nsm^{-2})
R_M= hydraulic resistance of the clean membrane (m^{-1})

2.4.1. Effect of temperature:

The membrane flux is strongly temperature dependant, as temperature influences the viscosity and density of water. Using the known relationship between viscosity and temperature, the following correction for flux at a standard temperature (20^0C) can be used (AWWARF, LdE, WRC, 1996):

$$J_{T=20\,C} = J_T \cdot e^{-0.0239(T-20)} \quad [2.2]$$

where T = temperature of system (^{0}C)

2.5. Filtration of solutions and suspensions

The solutions being filtered in an MBR contain high levels of suspended and dissolved material. The presence of these species will have a strong effect on the permeate flux. The permeate flux achieved for a particular solution depends on the membrane type and operating conditions used.

Fane and Fell (1987) and Howell and Finnigan (1991) conclude that the build up of membrane foulants occurs in two time intervals:

- Initial flux decline, which is due to the build up of a concentration polarisation layer. The presence of dissolved substances in the solution will cause an accumulation of solutes on the retentate side of the membrane.

- Long term fouling, which is due to solute adsorption and particle deposition (gel layer and cake formation). High concentrations of solutes at the membrane surface may cause precipitation forming a gel layer. Particles in suspension will be transported to the membrane surface and form deposits. This gel and/or cake layer will reduce the hydraulic permeability and thus reduce the permeate flux.

2.5.1. Initial fouling:

2.5.1.1.Concentration polarisation

As the solvent passes through the membrane and some of the dissolved species are rejected, a difference in concentration between the retentate and permeate side develops. This concentrated layer is less permeable for the solvent (water) compared to the bulk solution. Also, as the solutions on either side have different concentrations, they also have a different osmotic pressure. These two factors will cause a reduction in the flux relative to that of clean water.

The dissolved species are transported to the membrane surface with the bulk solvent. The concentration gradient within the boundary layer will be set up within the first few seconds of operation (Fane and Fell, 1987). The concentration gradient induces diffusion of the solute back towards the more dilute bulk solution. The system will quickly find a dynamic balance as shown in Figure 2.4.

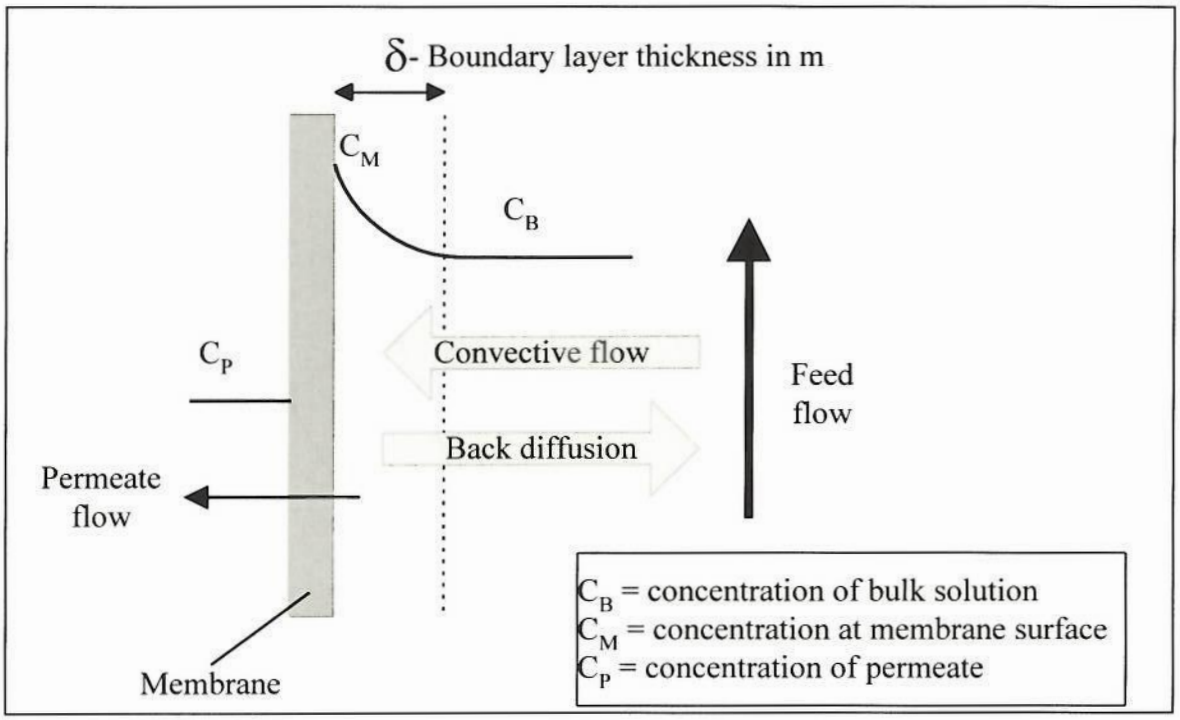

Figure 2.4 Concentration polarisation boundary layer

The flux reduction due to rejected solutes can be estimated using the osmotic pressure model or the boundary layer resistance model. These models are outlined below, and have both been verified in practice (Winston Ho and Sirkar, 1992)

2.5.1.2.Osmotic Pressure model

The concentration gradient near to the membrane surface causes a difference in osmotic pressure. This difference in osmotic pressure will act in a direction opposite to that of

the fluid driving pressure. Hence, for non-pure water solutions, equation [2.1] must be modified to give:

$$J = \frac{(\Delta P - \Delta \pi)}{\mu . R_M} \qquad [2.3]$$

where $\Delta\pi$ = osmotic pressure (Nm^{-2})

This relationship requires information on the relationship between concentration and osmotic pressure. However, this correlation information is not usually available for high molecular weight molecules. As these large molecules are major contributors to the concentration polarisation layer in UF and MF, this model may be difficult to apply to MBR design. Also, Green and Belfort (1980) state that the solution osmotic pressure is not significant for colloidal solutions.

2.5.1.3.Boundary layer resistance model

This method considers the hydraulic permeability of a concentrated layer at the membrane surface. The boundary layer thickness, δ in m, (as shown in Figure 2.4) is the distance over which the concentration changes from C_B to C_M. The distance δ is a function of flow and diffusion conditions.

The flux, J, is related to δ by:

$$J = k.\ln\left[\frac{(C_M - C_P)}{(C_B - C_P)}\right] \qquad [2.4]$$

where $k = D/\delta$ = mass transfer coefficient (ms^{-1})
and D = diffusion coefficient (m^2s^{-1})

As flux increases with increased pressure, C_M also rises. At limiting conditions, C_M will reach the solubility limit and precipitation will occur, leading to gelation. Further increases in pressure will not yield higher flux. When C_P is assumed to be small compared to C_M, equation [2.4] simplifies to:

$$J = k.\ln\left(\frac{C_M}{C_B}\right) \qquad [2.5]$$

The mass transfer coefficient, k, can be estimated from correlations of the Sherwood number in terms of the Reynolds number and the Schmidt number.

The Sherwood number, Sh, is related to the mass transfer coefficient by:

$$Sh = \frac{k.d}{D} \qquad [2.6]$$

where d = characteristic dimension of hydraulic system (m)
e.g. tube diameter.

The Reynolds number, Re, can be found using:

$$Re = \frac{d.\upsilon.\rho}{\mu} \qquad [2.7]$$

where υ = velocity of feed flow (ms^{-1})
ρ = fluid density (kgm^{-3})
μ = viscosity (Nsm^{-2})

and the Schmidt number, Sc, using:

$$Sc = \frac{\mu}{\rho.D} \qquad [2.8]$$

The correlation is of the form:

$$Sh = f^n(Re, Sc)$$

A more detailed account of this model including the constants used in this correlation can be found in Winston Ho and Sirkar (1992).

2.5.2. Long term fouling:

Suspended particles are also transported to the membrane surface with the solvent, and will be rejected if their size is greater than the pore diameter. Some of the particles will adsorb or be deposited onto the surface of the membrane. The mass of polarised solids will increase with time until the rate of deposition is balanced by the rate of shear-induced removal (Baker *et al.*, 1985). Figure 2.5 shows the form of the cake and concentration polarisation boundary layers:

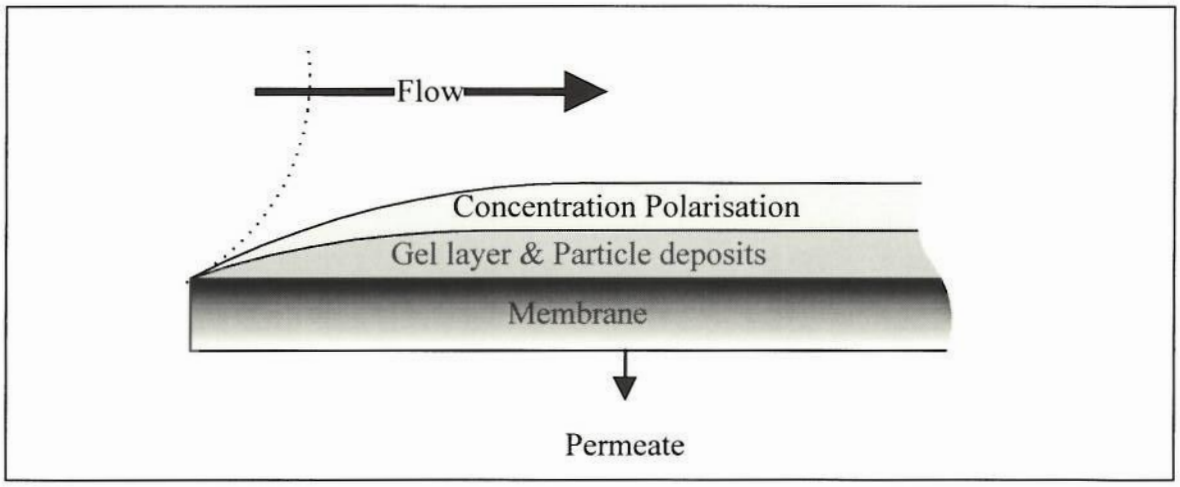

Figure 2.5 Cross flow filtration of solution containing suspended and dissolved material

These particulate deposits (filter cake) will give an additional resistance to solvent flow. The total resistance to solvent flow can be considered as the sum of the individual resistances. This technique, known as the 'Resistance in series' model (Persson and Nilsson, 1991), can be expressed as shown in equation [2.10].

$$J = \frac{\Delta P}{\mu . R_T} \qquad [2.10]$$

where R_T = total resistance to solvent transport, (m^{-1})
$= R_M + R_{CP} + R_G + R_C$

where R_M = Resistance of membrane, (m^{-1})
R_{CP} = Resistance of concentration polarisation layer, (m^{-1})
R_G = Resistance of gel layer, (m^{-1})
R_C = Resistance of solids cake formation, (m^{-1})

The resistance due to fouling can be combined in single term such that:

$$R_F = R_{CP} + R_G + R_C$$

The mechanisms by which particles are transported to the membrane surface are more complex than those for dissolved species. Unlike dissolved macromolecules, suspended particles are hydrodynamically active. Hence, the particles will be subjected to scouring effects from the bulk flow.

2.5.2.1.Colloidal and particulate fouling

Porter (1972) found that filtration rates were up to an order of magnitude higher for colloidal suspensions than solutions containing an equal mass fraction of

macromolecules. This result shows the different nature of the fouling layer in the two cases. Colloidal fouling has been modelled by several authors and a summary is shown in Table 2.4:

Table 2.4 Colloidal fouling models

Model description	Reference
Mass transfer equation linking hydrodynamics and suspension properties	Bacchin *et al.*, 1995
Surface renewal theory applied to membrane surface elements	Koltuniewicz and Noworyta, 1994
Standard blocking model and Cake filtration model.	Visvanathan and Ben Aim, 1989

Belfort (1989) describes two hydrodynamic models developed to explain the difference in fouling behaviour of suspensions and solutions, namely the 'moving cake' and 'pinch effect' models.

The moving cake model assumes that after a period of time where the fouling layer develops, the layer begins to flow across the surface of the membrane in the direction of the flow. As the particles do not have a high packing density, and are free to move and diffuse back to the bulk solution under the flow imposed shear, the resistance to permeation is lower. Macro-solutes will not be affected by the flow in this way.

The second theory assumes that the particles interact with the cross flow as individuals. The convection of particles to the membrane surface (due to the permeate flow) is balanced by the scouring effect of the cross flow to some extent. The balance found will depend on particle size distribution and hydrodynamics. The 'pinch effect' has been identified as a possible motive for the transport of the particles from the membrane wall back into bulk solution.

The pinch effect has been shown experimentally (Segre and Silbergerg, 1962) for a concentrated particle suspension flowing in a tube under laminar conditions. The particles congregate in an annular region located between the centre line and the wall. This leaves a particle-free zone around the walls. Whether this model is applicable to turbulent flow is not clear.

2.6. Factors affecting membrane fouling

The factors which affect the rate and extent of membrane fouling can be broken down into three broad categories (Fane and Fell (1987):

(i) Membrane type: The membrane material, pore size & distribution and module configuration.

(ii) Operating conditions: Factors such as pressure, cross flow velocity and turbulence.

(iii) Solution characteristics: The nature of both solvent and solute, concentration and nature of the bulk fluid.

These controlling factors are discussed in the following sections.

2.6.1. Membrane type:

Differences in membranes can be broken up into categories: Module configuration, physicochemical properties of the membrane material, porosity and morphology of the surface.

2.6.1.1.Module configuration

Membrane modules for water treatment are manufactured in different configurations: flat sheet in plate-and-frame or spiral wound modules, hollow fibre and tubular type. Table 2.5 gives a summary of the different characteristics for UF modules.

Table 2.5 comparison of different membrane element configurations - adapted from Winston Ho and Sirkar (1992).

Type	Feed channel height (mm)	Area packing density (m^2m^{-3})	Feed velocity (ms^{-1})	Reynolds number	Cost (£m^{-2})	Typical suppliers
Hollow fibre	1 - 2.5	1200	0.5 - 3.5	10 - 1,000	130-200	Amicon Romicon
Tubular	3 - 25	60 - 200	2 - 6	10,000 - 30,000	50-450	Koch PCI Wafilin
Plate-and-frame	0.3 - 1	300	0.7 - 2.0	100 - 6,000	50-130	DDS Millipore
Spiral wound	0.5 - 1	600	0.2 - 1.0	100 - 1,000	25-130	Fluid systems Koch

The size of the feed channel is an important consideration when filtering a solution with high suspended solids. Winston Ho and Sirkar (1992), state that solids will cause plugging of the element if the average size of particles is greater than 1/10 of channel dimensions. The channel dimensions also affect the flow regime within the module for a given flow rate.

2.6.1.2.Membrane material

The membrane material has a strong influence on the quantity of material adsorbed onto it's surface. Wakeman (1996) states that the hydrophobicity of the material affects fouling characteristics, particularly during the early stages of fouling.

The adsorption of material onto a surface is subject to electrostatic forces. The likelihood of adsorption of the particle will be affected by the surface charge of the membrane. However, Wakeman (1996) states that for filtration of suspensions the surface charge has only a minor effect on flux decline.

2.6.1.3.Porosity and morphology of the membrane surface

The porosity of the membrane surface will affect the pressure required to produce a certain flux. The porosity of UF membranes can vary according to material and method of manufacture. Fane and Fell (1987) report values of 0.3 - 15% surface porosity in previous studies. This contrasts with MF membranes which have a typical porosity of 75 - 85%.

The low porosity of UF membranes means that solvent flowing towards the membrane does not meet a homogeneously permeable surface, but will have to follow streamlines to the opening of isolated pores. This may increase local concentration polarisation. Hodgson and Fane (1991) found that a 0.02μm Anopore membrane with a porosity of 35% gave a higher flux than a 0.2μm Ceramesh membrane with a porosity of 20%. The solution filtered was a bacterial broth and a trans-membrane pressure of 1 bar applied.

Another factor affecting fouling tendency is the pore size distribution. The likelihood of pore blocking depends on the relative sizes of particle and pore. A solution containing particles with an average diameter comparable to pore size is more likely to cause blocking.

2.6.2. Operating conditions:

2.6.2.1.Hydrodynamics

The convection to and diffusion away from the surface of the membrane affects concentration polarisation and gel layer formation. The adsorption and deposition of

particulate matter is also governed by the balance of forces to and from the membrane surface.

The rate of convection to the membrane surface is a function of the permeate flux, and the diffusion of solutes away from the surface is determined by the mass transfer coefficient (k). The mass transfer coefficient increases with increasing Reynolds number, Re, as described in Section 2.5.1.3.

Many techniques have been used to control and modify the hydrodynamic behaviour in the membrane element. Details of some of these methods are given in Section 2.7.4.

2.6.2.2.Pressure

For pure water, equation [2.1] shows that flux is directly proportional to trans-membrane pressure, ΔP. When a suspension or solution is filtered, this linear relationship will apply while the resistance due to fouling is small compared to the membrane resistance (equation [2.10]). As the resistance of the fouling layer predominates, flux becomes independent of applied pressure. The ΔP at which flux ceases to increase with increasing pressure is known as the critical pressure, ΔP_C (Howell, 1996).

Operating the system above this critical pressure will cause gel layer compacting and consequently lower flux. Increasing the trans-membrane pressure to regain the lost flux will succeed for a short period only, as the system will be unstable and flux will subsequently decline.

2.6.3. Solution characteristics:

Research has shown that the solution characteristics have a strong influence on fouling. Wakeman (1996) states that the most important regarding flux decline are: Solids concentration, pH and particle size distribution. During the filtration of biological solutions, the micro-organisms present can also have an influence on flux (Hodgeson *et al.*, 1993).

2.6.3.1.Solution concentration

A solution with a high concentration of suspended solids exhibits different behaviour to that of pure water. The suspended solids will alter the density and viscosity of the bulk fluid. The hydrodynamics inside the membrane element are described in terms of the Reynolds number, which is a function of both density and viscosity. Hence, the concentration of the feed solution must be taken into account when calculating the flow regime.

Krauth and Staab (1994) developed a relationship between the solids concentration, viscosity and density of the feed solution, when using activated sludge with an MLSS concentration between 2,500 - 3,500 mgl^{-1}.

This relationship can be used to determine a modified Reynolds number, Re', which takes into account the SS present. This can be written as:

$$Re' = \upsilon \cdot d \cdot \rho' / (\eta' * 10^{-3})$$

where:

$\rho' = \rho_w * (1.000145+0.000236*MLSS+0.00001296*MLSS^2+0.0000001758*MLSS^3)$

and

$\eta' = \eta * 1.044625*e^{0.08.1151*MLSS}$

Figure 2.6 shows how these relationships affect the modified Reynolds number. The graph has been plotted using a value of 998.2 kgm^{-3} for clean water density, $1.002 * 10^{-3}$ Nsm^{-2} clean water viscosity (Metcalf and Eddy, 1991) and a characteristic dimension of 12mm (e.g. for a tubular membrane diameter).

The line at an Re of 4000 shows where the change from a laminar to a turbulent flow regime is normally considered to occur for flow in a porous tube (Belfort, 1988).

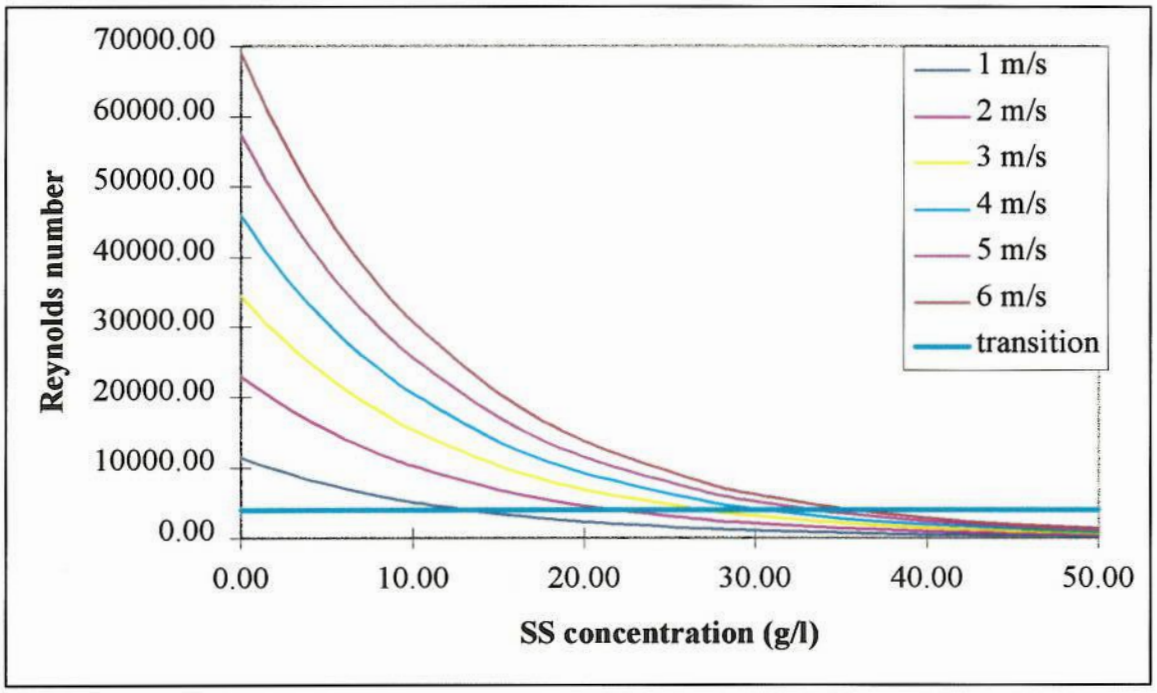

Figure 2.6 Effect of SS concentration on Re for different cross flow velocities

Figure 2.6 shows that as SS concentration increases, the velocity must be increased to maintain turbulent flow. If the MBR is designed to have an MLSS of 30,000 mgl^{-1}, the crossflow velocity must exceed 4 ms^{-1} to achieve a turbulent flow regime.

As stated in Section 2.1, one of the advantages of MBRs is the high MLSS which can be maintained in the reactor. As the mixed liquor is passed through the membrane, this high SS concentration has an effect on the fouling characteristics and hence the flux decline.

Beaubien *et al.* (1996) found a linear relationship between stabilised flux and MLSS in an anaerobic bioreactor. The flux through a 0.2μm ceramic tubular membrane was found to decay from 13μms^{-1} @ 2,500mgl^{-1} to 7μms^{-1} @ 22,000 mgl^{-1} MLSS concentration.

Al-Malack and Anderson (1997) found a linear relationship between steady state permeate flux and the natural logarithm of solids concentration. The study was based on secondary waste water filtered through a dynamically formed membrane on a woven multi-filament polyester yarn (20-40 μm pore size).

Wang Shu-Sen (1988) investigated the relationship between permeate flux and solution viscosity. Four different solutions were used: Glycerine, Bovine serum albumin, polyethylene glycol and raw rice wine, and three distinct relationships were reported. At low viscosity (1 - 3 $mNsm^{-2}$), a small increase in viscosity produced a very large drop in flux. At medium viscosity (3 - 6 $mNsm^{-2}$), flux decrease was moderate with increasing viscosity. At high viscosity (> 6 $mNsm^{-2}$), permeate flux was almost independent of solution viscosity.

Bertram *et al.* (1993) found an increasing filter cake resistance for increasing solution concentration. The experiments were performed on a silica suspension (500 - 1,500 mgl^{-1}) using a sintered aluminium membrane narrow tube 0.2μm microfilter-.

Magara and Itoh (1991) determined an empirical relationship between SS concentration and permeate flux through a UF membrane. The solution was taken from a biological reactor and the SS ranged from 5,000 mgl^{-1} to 12,000 mgl^{-1}. The cross flow velocity was not stated, and the trans-membrane pressure was 0.3 bar. The relationship found can be written:

$$J = -1.571 \log (MLSS) + 7.84$$

where J = flux in $m^3m^{-2}day^{-1}$
MLSS in mgl^{-1}

2.6.3.2.Solution pH

Solution pH affects the charge and solubility of many solutes. The surface charge of the solutes provides a repulsive force between them which prevents aggregation. At the isoelectric point (IEP) the repulsive force is zero, aggregation occurs and the likelihood of deposition as fouling is increased. Solution pH can therefore affect the likelihood and extent of fouling (Wakeman, 1996).

A change in pH can also result in decreased osmotic pressure (Van den Berg and Smolders, 1990) and can postpone gelation by allowing an increase in gel concentration.

2.6.3.3.Particle size distribution

Baker *et al.* (1985), found that the lateral migration of particles from the membrane surface was dependant on particle size and flow velocity. When cross flow velocity was increased, the mass of cake deposited on the membrane surface was found to be less. However, the resistance to filtration per unit mass of cake was increased. This was interpreted as the cake containing smaller particles with a higher packing density and corresponding lower porosity.

2.6.3.4.Microbial suspensions

The adhesion of micro-organisms to the membrane surface during cross flow filtration is a complex process. Defrise and Gekas (1988) provide a good summary of the models which have been developed to describe the effect. The main difficulty in finding a comprehensive model is the subtle interactions between cell and membrane surface.

Hodgson *et al.* (1993) investigated the effect of a microbial layer on the surface of the membrane during the filtration of bovine serum albumin. The influence of the cell surface properties on resistance and rejection were recorded. The authors concluded that the mechanism by which cake resistance and solute rejection occurs depends on the extracellular matrix of the organisms. This extracellular material contains complex polymers such as proteins and acidic polysaccharides.

The role of protein adsorption and salt precipitation has been investigated by Hanemaaijer *at al.* (1989). They found that solute-membrane interactions had a considerable effect on the separation characteristics, and that much of the adsorption occurred within the membrane structure. This leads to pore size reduction and higher resistance to permeate flow.

2.7. Methods of amelioration of fouling

There are many methods of addressing the problem of fouling in the design of membrane filtration systems. The factors affecting fouling have been detailed in the previous sections, and in the following sections techniques which have been found to reduce or prevent fouling are summarised.

2.7.1. Membrane cleaning:

During the filtration of solutions and suspensions using UF and MF membranes a gel or cake layer is normally formed on the surface of the membrane. As this fouling layer increases the flux declines. When the flux declines below a certain level it will become uneconomical to continue the process. At this point it is common to apply some kind of cleaning regime to the membrane surface.

For membranes made of a rigid material e.g. ceramic tubular type or some hollow fibre modules, backwashing may be possible. This involves forcing clean water (or clean water and air mixture) from the permeate side to the retentate side. This technique has been used in several studies, notably Fane and Fell (1987) using Memtec hollow fibres. The other membrane configuration for which a physical cleaning method is applied is a tubular element. In this case various materials (e.g. sponge balls) have been passed through the element. This reduces the fouling layer with a scouring effect.

With most other membrane modules, fouling removal must take place by passing a cleaning solution across the retentate side. Cross (1991) investigated the effect of different cleaning solutions on the flux recovery after cleaning. Different membrane configurations (flat sheet and hollow fibre), from different membrane manufacturers were used in the study. He concluded that the efficacy of the cleaning process was dependant on duration as well as solution formulation.

Chemicals commonly used for membrane cleaning include: alkalis, acids, chlorine, surfactants, enzyme active solutions and bactericides (Cross, 1991). The choice of cleaning solution will normally be restricted by the chemical resistance of the membrane material.

2.7.2. Membrane surface modification:

Modifications to the surface of the membrane have been reported to reduce the build up of a fouling layer. A summary of some techniques which have been found to improve flux is shown in Table 2.6:

Table 2.6 Membrane surface treatment techniques used to increase flux

Technique	Reference
Charged membranes	Shimizu *et al.*, 1989
Pre-coating of membranes with surfactants	Fane *et al.*, 1985
Electric fields	Bowen *et al.*, 1987
Immobilised enzymes	Wang *et al.*, 1980 Velicangil and Howell, 1981 Gregor and Gregor, 1978

Fane and Fell (1987) state that the ideal UF membrane for most applications would be hydrophilic. Using a polysulphone membrane treated with a non-ionic surfactant (to increase hydrophilicity) less flux decline was observed than for an untreated membrane. Attaching hydrophilic chains to a hydrophobic membrane has been found to increase flux during ultrafiltration of protein (Van den Berg and Smolders, 1990).

2.7.3. Solution modification:

The electrostatic repulsion between particles in solution and between particle and membrane may have an effect on the fouling nature. Following this theory, Wakeman (1996) has suggested altering the solution to maximise repulsion and hence minimise fouling. The electrostatic forces between particles can be maximised by pH control.

This chemical treatment may not be practical if the metabolism of the biomass is adversely affected. Metcalf and Eddy (1991) state that the pH should be in the range 5 - 9 to maximise biological activity in an aerobic reactor, and 6 - 8 for anaerobic treatment.

2.7.4. Hydrodynamic modification:

In order to increase wall shear and scour the membrane surface, many techniques have been investigated. Methods which have been applied to commercial modules include: increased axial flow rate (laminar to turbulent), physical inserts, Taylor vortices, pulsed flow and combinations of these (Belfort, 1988).

2.7.4.1.Increasing cross flow velocity

Increasing the Reynolds number to create turbulent flow can be done directly by increasing velocity. Investigations have shown that increasing flow velocity yields an increase in flux, as shown in Table 2.7.

Table 2.7 Relationship between cross flow velocity and flux in previous studies

Membrane	Pore size / MWCO (μm / Daltons)	Velocity range (ms^{-1})	Flux range ($lm^{-2}h^{-1}$)	Reference
Polyester, tubular dynamic layer	20-40	1.2 - 1.9	3 - 14	Al-Malack and Anderson (1997)
Polysulphone,	20,000	1.1 - 2.2	15 - 35	Magara and Itoh (1991)
PSF, tubular	0.04	1 - 6	10 - 200	Krauth and Staab (1993)
Ceramic, tubular	300,000	1 - 4	50 - 225	Cicek et al. (1998)

This can be ascribed to two processes:

- An increase in mass transfer away from the membrane surface, hence reducing concentration polarisation.
- A reduction in particulate fouling due to increased shear rates and scouring action at membrane surface.

For a given membrane module, an increase in cross flow velocity can be achieved by increasing flow rate through the module. Consideration should be given to the flow regime during design, as module geometry will determine the cross flow velocity for a particular flow rate.

The headloss through the membrane system is a function of the cross flow velocity and the solution viscosity. Higher flow velocities can be used to create a turbulent flow regime. However, in the turbulent regime, velocity is proportional to pressure drop squared. Higher pressure drop across the module leaves less pressure available to drive filtration. Higher flow velocities require more energy for pumping, and return a lower recovery ratio of permeate flow/feed flow (Mikulasek, 1994).

2.7.4.2.Turbulence promoters

Another method of increasing the mass transfer and shear effects is by the use of turbulence promoting baffles prior to, or inside the membrane element. Field *et al.* (1995) reports an increase of 100% in the steady state flux using a helical baffle. The baffle was placed inside a 0.14μm tubular MF element during filtration of 5% dry weight yeast solution.

Howell and Finnigan (1991) conclude that the use of turbulence promoters should be undertaken with regard to the following:

- The improvement in flux and reduction in flux decay is dependant on the Reynolds number, Re. This Re dependency is system and/or feed specific.
- The optimum spacing between turbulence promoters and the optimum distance from the membrane depends on the flow configuration.
- Typically, these devices occupy a large volume fraction of the feed channel (20-50%). Hence, the frictional pressure drop associated with the module can be increased by a factor of several hundred - resulting in lower volumetric flow rates. With a turbulence promoter in place, the flux can be equivalent to that produced at far higher velocities in a standard element. Operation at lower velocities may negate this increase in pressure drop.

A novel technique reported by Arroyo and Fonade (1993) involves the use of intermittent jets to create vortices in the flow. This is achieved by placing a nozzle co-axially within the membrane feed line. Under normal control the feed flows around the nozzle. Periodically the flow is routed through the nozzle which results in a velocity step, generating a toroidal vortex which travels along the membranes length. This technique resulted in slower flux decline and over 100% increase in final flux.

2.7.4.3.Rotating membranes

Another method for providing an additional shear force on the surface of the membrane is the rotating membrane. The membrane module is made up of two concentric tubes, one inside the other. The feed solution flows in the annulus between the two tubes and the permeate passes through the membrane which surrounds the feed channel. The inner tube is rotated at high speed which causes flow instabilities resulting in Taylor vortices. These vortices create a shearing mechanism, whose major advantage is its independence of feed cross flow velocity.

Kroner and Nissinen (1988) concluded that an axially rotating filter improves the performance of cross flow microfiltration of microbial suspensions. The flux produced from this type of filter increases with increasing speed of rotation.

2.7.4.4.Pulsed flow

The use of time varying feed flow characteristics to enhance permeate flux has been investigated by several authors. Bertram *et al.* (1993) provides a summary of the possible mechanisms which cause an increase in cross flow filtration efficiency.:

- The root mean square (rms) magnitude of the viscous shear at the membrane surface can be increased, improving fouling and concentration polarisation reduction. If the frequency of pulsation is sufficient, the instantaneous velocity profile can be disturbed. This further increases the rms shear.

- During the flow retardation part of the cycle, turbulent mixing can occur at the membrane surface even during laminar flow. This will improve the mass transfer back to the bulk solution.
- Under certain conditions, during the flow pulsation the instantaneous trans-membrane pressure may become negative. This can cause a backwashing effect from the permeate side leading to foulant removal.

Table 2.8 shows the flux increases found during previous studies:

Table 2.8 Increase in steady state flux due to flow pulsation

Membrane	Solution	Steady state flux increase %	Reference
MF, 0.2μm Ceramic, Tubular	silica suspension	60	Bertram *et al.* 1993
Hollow fibre.	Plasma	45	Jaffrin *et al.* 1987
UF Flat sheet	albumin	25 - 300	Rodgers and Sparks, 1991

Another technique using periodic pressure variations has been investigated by Boonthanon *et al.* (1991). This method employed a system of valves to close the permeate line and feed line while opening a by-pass line. The timing of these valves was varied and the effect on permeate flux recorded. Improvements of up to 80% were seen in permeate flux. The authors concluded that the improvement was due to disturbance of the fouling layer by the shock waves and feed flow changes.

2.7.4.5.Combinations

Having seen improvements in flux due to pulsatile flow and turbulence promoters independently, Finnigan and Howell (1989) set up an experiment combining the two effects.

The experiment used a modified pump giving pulsatile flow with a frequency of 2.5 Hz, and ring shaped baffles inside tubular UF membranes. The flux was compared with conventional flow through the module. The increase in flux reported was 236-268%. The increase in power consumption due to the pump and pressure drop across the baffles was found to be small in comparison with the flux increase.

2.7.5. Sub critical flux operation:

Under certain operating conditions, some authors report a stable long term flux during MF and UF membrane filtration of solutions. Howell (1995) has performed many studies on the concept of critical flux. The theory behind sub critical flux operation centres on the trans-membrane pressure, ΔP.

For pure water, the flux increases linearly with increasing ΔP according to equation [2.1]. When filtering a suspension, initially the flux will respond to increasing ΔP in the same way. As ΔP exceeds a certain value, the flux deviates from the linear response, see Figure 2.7. This is known as the critical pressure, ΔP_C.

When filtering anaerobic biomass suspensions, Elmaleh and Abdelmoumni (1997) found that steady state flux reached a maximum at a driving pressure of around 1 bar gauge. After this maximum, the flux actually dropped away slowly. These results were obtained using four different tubular MF and UF modules, at a SS concentration of 1300 mgl^{-1}.

Operating the membrane with $\Delta P < \Delta P_C$ should result in a stable long term flux (Howell, 1995, Field *et al.*, 1995).

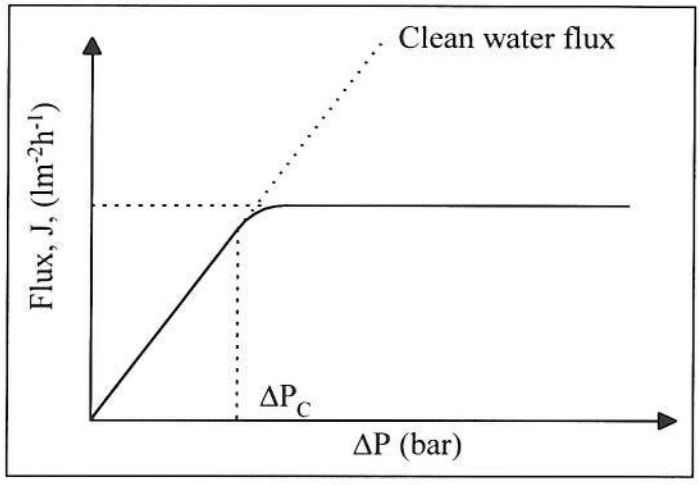

Figure 2.7 Illustration of critical trans-membrane pressure

The permeate flux achieved during this mode of operation is below the maximum attainable due to the low trans-membrane pressure. However, removing the need for cleaning is a major advantage due to reduced costs.

The sub critical flux is low, and therefore requires a relatively large membrane area to produce a given permeate flow rate. However, the reduction in cleaning pipe-work complexity will go some way to redress the financial balance. Additionally, removing the need for cleaning chemicals and the reduction in down time makes the decision more balanced. It is also common practice to use the permeate product water in any cleaning or backwashing process. The portion of product water varies, though it can be substantial.

2.8. Cost drivers in MBR systems

Many parameters affect the cost of constructing and operating an MBR system. The desired biological characteristics will affect both the investment costs and the operating costs. The cost of the membrane filtration step will also be affected by the biomass characteristics. The hydrodynamic conditions used in the filtration will not only determine the energy consumption, but also affect the fouling characteristics. The interdependency of these factors is summarised in Figure 2.8.

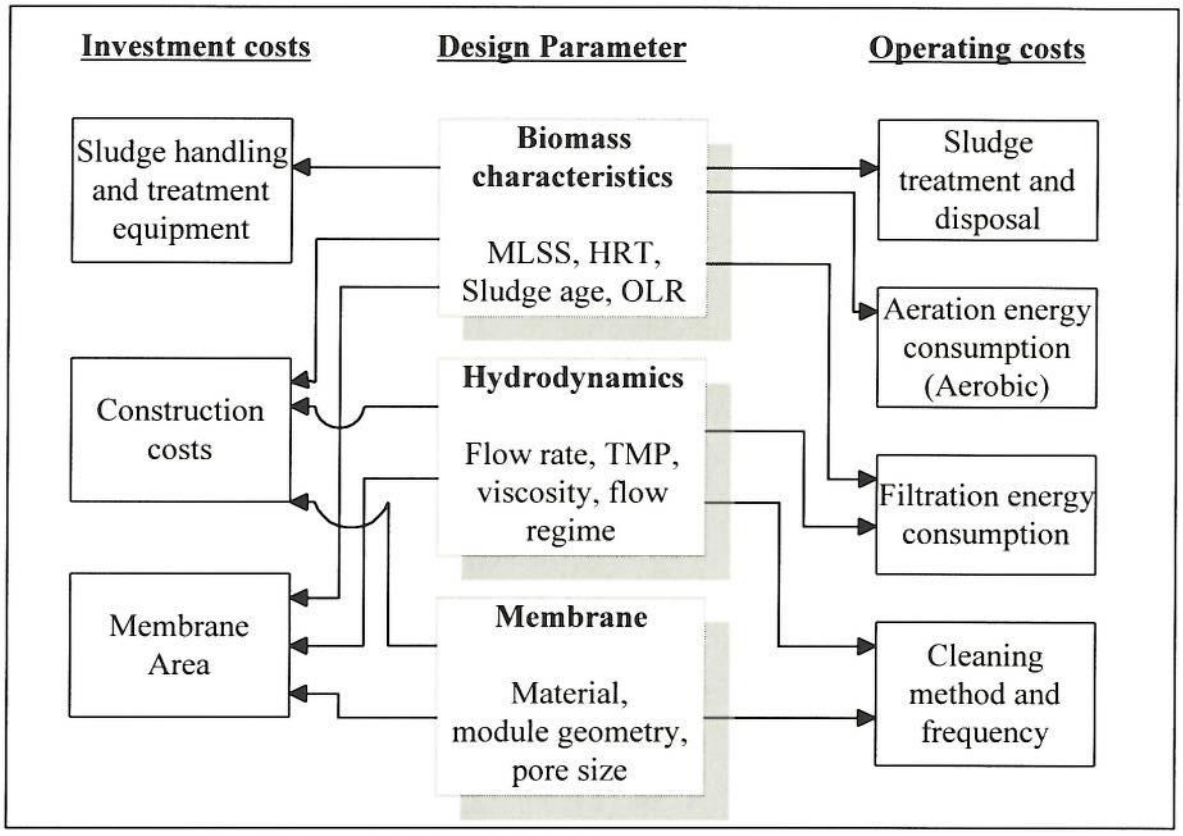

Figure 2.8 Interdependency of membrane filtration parameters (Adapted from AWWARF, LdE, WRC, 1996)

A useful measure of the operating costs of running the membrane plant is the power consumption per unit permeate produced ($kWhm^{-3}$). Table 2.9 shows the values found in some previous studies.

Table 2.9 Operating costs for different membrane systems

Membrane type and configuration	Wastewaster	Power cost $kWhm^{-3}$	Reference
UF, 0.04μm Ceramic Tubular	Industrial	8 - 27*	Krauth and Staab, 1993
MF, 0.1μm PE Hollow fibre Integrated MBR	Domestic	1.5 - 3.0	Ueda et al., 1996
UF	Domestic	10 - 25*	Magara and Itoh, 1991
Conventional Biological Treatment system	Municipal	0.2 - 0.3	Ueda et al., 1996

* Filtration costs only

These operating costs are higher than those incurred during conventional solid/liquid separation during wastewater treatment. The increased costs must be balanced by the advantages detailed in Section 2.1. For example, a reduction in sludge production will reduce sludge treatment and handling costs.

The published data on energy consumption (Table 2.9) shows the lowest values reported by Ueda *et al* (1996). This shows the advantage of the integrated MBR system. As the membranes are inside the reactor, it is not necessary to employ recirculating pumps - these being the major energy consumer in a side stream system. However, due to the low flux produced from the membranes used for an integrated system, the membrane area required will be high. This will increase the capital cost of the plant (Owen *et al.*, 1995).

3. AIMS AND OBJECTIVES

The principal objectives of this study have been to investigate the fouling characteristics of different membranes under a range of operating conditions.

Initially, the flux produced by each membrane will be investigated under increasing pressure while filtering clean water. This will indicate the hydraulic resistance of each membrane.

Using waste water, the stabilised permeate flux will be investigated under the following conditions:

- Three membrane types
- Three feed solution concentrations
- Three cross flow velocities.

With the optimum cross flow velocity (in terms of flux produced per unit pressure) identified, a further comparison is to be made comprising:

- Three membrane types
- Four feed solution concentrations

The results of these investigations will indicate the most economical arrangement for a particular solution concentration. These results are to be used to estimate the power cost per unit permeate produced, and hence the most economical operating regime under the conditions investigated.

Operation of the membranes in the sub critical flux region will be investigated. The trans-membrane pressure minimised and long term runs undertaken. Dynamic stabilisation of the fouling deposits will be indicated by a stable flux and trans-membrane pressure.

A novel method for fouling control is to be investigated. This technique involves a periodic increase in cross flow velocity to reduce cake layer build up.

During the experiments, the feed solution and the permeate will be analysed for key contaminants. This will assess the selectivity of the membranes under different conditions and indicate product water quality.

4. EXPERIMENTAL

4.1. Rig description

A pilot rig was used to investigate the fouling characteristics of membranes performing the solid-liquid separation step of a membrane bioreactor. As the physical separation process was to be the focus of the study, the rig was designed to draw biomass from an existing biological reactor. This would give a stable source of biomass, and avoid the delays and problems associated with starting up and controlling a pilot reactor.

The experimental rig was designed by John Gibson (Anglian Water Services Ltd) and constructed by Waterlink Ltd. The control system was supplied and installed by Environmental Control Systems (Anglia) Ltd, who also carried out the commissioning.

Figure 4.1 shows a photograph of the pilot rig. It consists of two parallel streams with a shared feed tank and chemical cleaning tank.

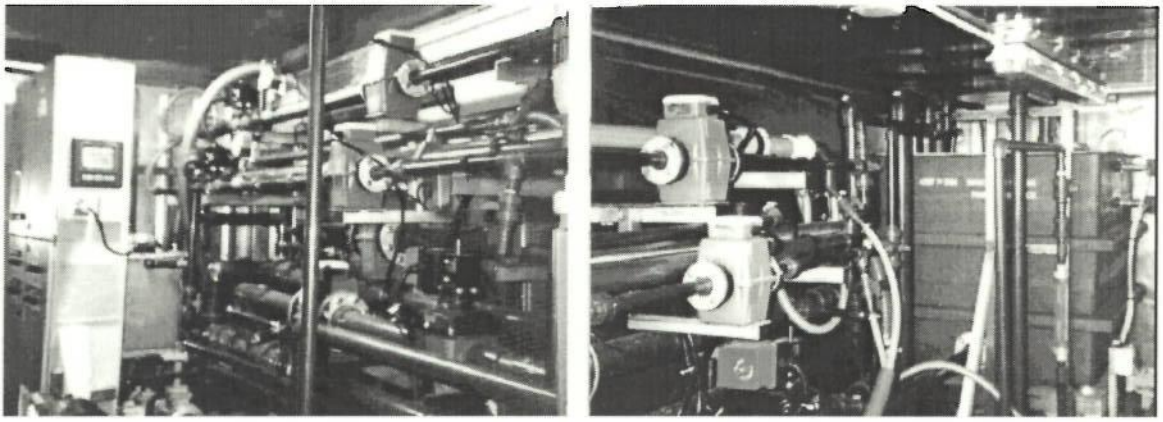

Figure 4.1(a) and (b) Photographs of the pilot plant

In the background of Figure 4.1(a), the control panel and data-logger can be seen. The pipe-work, valves, flow meters and membrane modules occupy the centre. In Figure 4.1(b), the sludge feed tank can be seen in the background with its level switches. The light coloured M2 membrane module can be seen behind the upper flow meter.

Figure 4.2 shows a schematic with component details for stream 1. Component details for stream 2 are shown in Figure 4.3.

The feed tank, which has a nominal volume of 1 m^3, acts as a reservoir for the sludge. As the retentate flows back into the feed tank, the sludge is kept well mixed by the turbulence created. Each stream can accommodate one membrane module of up to 3m in length. The two streams can be run simultaneously or independently. The overall

dimensions of the rig structure are approximately: 5m x 1.5m x 2m, and it is housed in a mobile container.

4.1.1. Pipe-work:

The pipe-work on the rig is fabricated from 'E' grade PVC plastic (BS 4346/1) which is suitable for pressures of up to 9 bar gauge. The main streams carrying sludge from the feed tank to the membranes and returning to the feed tank are 3" diameter. The permeate lines and cleaning solution lines are 1" diameter.

4.1.2. Pumps:

The pumps used for supply and wastage of sludge, and those providing the membrane feed flow are all MONO pumps operating through Leroy Somer gearboxes. Details are shown in Table 4.1 below:

Table 4.1 Pump details

Location	Make, model etc
Sludge in/out of feed tank	MONO, CBOX1AC1R4/G 0.5 bar
Main membrane feed pumps	MONO, CB081AC1R4/G
Cleaning solution recirculation	MONO, CGH113R3

4.1.3. Monitoring equipment:

The Table below lists details of the measuring devices used on the experimental rig:

Table 4.2 Monitoring equipment details

Instrument	Make, model and specification
Electromagnetic flow-meters	ABB Kent-Taylor, MagMaster 50mm
Rotameter flow-meter	Krohne VA 20 K
Pressure gauges	Bourdon Sedeme 0 - 6 bar
Data-logger	Penny & Giles - Trend View Multitrend 8 channel

The Penny & Giles data-logger receives analogue inputs from eight sources. These are the four pressure gauges, PG 1 to 4, and four flow meters, FME 2, 3, 5 & 6. The analogue inputs are converted to digital form, and represented in their engineering units.

The data-logger can display and record up to nine data series. Simple algorithms were performed on some of the data streams before they were displayed and recorded:

- The flow meter inputs were displayed and recorded 'as such'.
- The inputs from PG 2 and PG 5 were subtracted from PG 1 and PG 4 respectively, giving two data sets representing the trans-membrane pressure for each stream.

- The inputs from FME 2 and FME 5 were combined with inputs from PG 1 and PG 4 to give an estimate of the energy consumption during operation.

The expression used to estimate power used (in Watts) can be written:

$$\text{Power } (Nms^{-1}) = \text{Flow } (m^3s^{-1}) * \text{Pressure } (Nm^{-2})$$

The energy consumption per unit permeate is found using:

$$\text{Energy consumption } (kWhm^{-3}) = \frac{\text{Power (W) / 1000}}{\text{Permeate flow rate } (m^3h^{-1})} \quad [4.1]$$

The data from each source was averaged and logged every two minutes during most runs. During some short duration trials the information was logged every 30 seconds.

4.1.4. Control equipment:

The rig is semi-automated, and proceeds under PLC control once a run is initiated. Details of the control equipment are shown in the Table below:

Table 4.3 Control equipment on pilot plant

Component	Make & model
Motorised valves	Valpes
Variable speed pumps	MONO pumps, Leroy Somer Gearing
Pump speed controller system	Honeywell CXS0075
Feed tank level switches	Floatec
Cleaning solution tank heater	Heatex HBY 311/A 3 kW
Cleaning solution tank level switch	Vega Swing 71A.XGAVXST

4.2. Membranes used

Three different types of membrane have been investigated, details of which are shown in Table 4.4.

Table 4.4 Specifications of membranes used during trials

Code	Manufacturer	Material	Configuration	MWCO (kDa)/Pore size (μm)	Total membrane area (m^2)
M1	PCI	PVDA	12mm tubular	250	2.23
M2	Koch	PVDF	12mm tubular	250	2.23
M3	Koch	PVDF	12mm tubular	0.1	2.23

As the membranes are housed in similar modules, direct comparison of their performance can be made. The M2 membrane module is shown below in Figure 4.4, the others being similar:

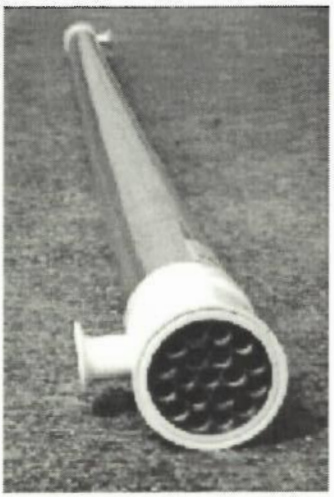

Figure 4.4 M2 membrane module

4.3. Sludge feed

The feed tank is fed from an external source via 2" flexible hosing. The source of the feed sludge was the Biological Nutrient Removal (BNR) plant at the Anglian Waste Water Innovation Centre, Cambridge. Sludge was taken from two points on the plant: The aerobic liquor recycle line and the settled sludge return (RAS) line.

The aerobic recycle mixed liquor has a suspended solids (SS) concentration of approximately 2,500 mgl^{-1}. The returned settled sludge has a SS concentration of approximately 7,500 mgl^{-1}.

By careful mass balance of flow into and out of the tank, the concentration can be controlled and held at any desired concentration. The SS concentration can be increased by using the membranes as sludge concentrators. If it is assumed that the permeate contains negligible SS, then by wasting the permeate to drain and replenishing the feed tank with fresh sludge, the concentration in the tank will rise. The time taken to reach the desired concentration is given by a spreadsheet as shown in Appendix A.

Maintaining the feed tank at a higher concentration to that of the influent sludge involves a more subtle balance, and requires that the flow of permeate to drain is known. To aid this process, a spreadsheet was set up to give the required flow into the tank for the desired concentration. The spreadsheet is detailed in Appendix A.

4.4. Rig operation

4.4.1. Pre-programmed routines:

The control system for the rig has three pre-programmed routines. Once initiated, the plant will run under programmable logic controller (PLC) control until it is shut down. The three routines which can be used are:

- Declining permeate flux mode
- Constant permeate flux mode
- Periodic flush mode

The declining flux mode has been used predominantly during these trials. The user defined variables for this mode are the feed flow rate and the maximum permissible trans-membrane pressure. The run will proceed with the desired feed flow rate and the permeate line valves (MBV 2&5) open. This mode was used to investigate the fouling characteristics with time, and can be run for any length of time as long as the trans-membrane pressure remains within the pre-set safety limit.

During the constant flux mode, the user inputs required are the feed flow rate, the required permeate flow rate and the maximum permissible trans-membrane pressure. The run proceeds at the set feed flow rate, and opens the permeate line valves (MBV 2&5) enough to allow the required permeate flow. Should the required permeate flow not be achieved with the valve fully open, the feed line valve (MBV 1&4 down stream of the membrane) will slowly close - increasing trans-membrane pressure - until the required flow is realised. This mode will run indefinitely as long as ΔP remains below the pre-set threshold.

The periodic flush mode is used to test a novel fouling reduction technique. The user inputs required are: feed flow rate; flush flow rate; flush duration; flush periodicity and maximum trans-membrane pressure. The run will proceed as with the declining flux mode. However, at pre-set intervals, the permeate line valve (MBV 2&5) will close and the feed flow rate will be increased to the flush flow rate. This flushing cycle will continue for the flushing duration specified, after which the permeate valves re-open and the feed flow rate is returned to normal. This mode will run indefinitely as long as ΔP remains below the pre-set threshold.

4.4.2. Safety features:

To initiate all three modes, the maximum permissible ΔP must be entered. Should this pressure be exceeded an alarm will sound and the stream will partially shut down. This prevents damage to the membranes and reduces the likelihood of leaks caused by excess pressure.

During commissioning, it was found that the hose connections onto the membrane modules were prone to leaks should the ΔP rise above four bar gauge. As the rig was run unattended, the maximum permissible ΔP was set to 3.5 bar for all declining flux runs.

The feed tank was fitted with an emergency low level float switch. Under normal circumstances, the level was maintained at between 0.8 - 1m^3 by the waste pump (FSP 1). In the event of a feed pump failure, or a major leak, the entire system would be shut down before the main recirculating pumps (VSP 2 & 3) ran dry.

4.4.3. Feed flow rate:

The flow rate at which the main pumps (VSP 2 & 3) recirculate the sludge through the modules is a key operating parameter. The flow rate through the modules determines the cross flow velocity across the surface of the membrane. The flow rate also determines the pressure drop across the module, and hence the trans-membrane pressure.

For these trials, three flow rates were used: 300, 400 and 500 $lmin^{-1}$. These flow rates correspond to cross flow velocities in the membrane tubes of: 2.3, 3.1 and 3.9 ms^{-1}. For the flushing mode, a flush flow rate of 450 $lmin^{-1}$ was used, corresponding to a velocity of 3.5 ms^{-1}.

4.4.4. Membrane cleaning method:

Before each run, the membranes were chemically cleaned to ensure similar starting conditions. The chemical tank shown in Figures 4.2 and 4.3 is used to make up the solutions used. During the cleaning process, the rig must be shut down, and the pipe-work around the membrane isolated. This is achieved by closing the ball valves upstream of the membranes (BVH 7&8) and checking that the motorised valves (MBV 1 & 4) have closed on terminating the run.

Consideration must also be given to the volume of pipe-work which is used during the cleaning process. The volume of the chemical tank is approximately 60 litres. The 'hold up' volume of the pipe-work is approximately 40 litres. Hence, to maintain the solution at the desired concentration, a volume of 100 litres must be used in the calculations.

The cleaning regime is detailed below:

1. Clean water flush for 10 minutes at 50^0C
2. Caustic flush for 15 minutes at pH 10.5, temperature 50^0C
3. Hypochlorite clean for 15 minutes, pH 10.5, 200 mgl^{-1} free chlorine, temperature 50^0C.
4. Clean water flush for 15 minutes.

This regime must be applied to both membranes. To reduce the amount of chemicals used during the cleaning cycle, a recirculation loop was used. The hose connections from BVH4 and BVH6 were drained back to the chemical tank. This enabled the temperature to be kept at 50^0C and the concentration of the cleaning solution to be monitored more accurately.

The temperature was measured using a 'Whatman Thermopen' thermometer.

The pH was increased using 32% NaOH solution, and measured with a 'pHep' pH meter manufactured by Hannah Instruments Ltd. This meter has a resolution of 0.1pH and the quoted accuracy is ±0.2pH.

The hypochlorite used was 14-15% Sodium Hypochlorite solution. The free chlorine concentration was calculated by mass balance and verified using a HACH free chlorine pocket calorimeter (DPD Colorimetric method, Section 4-63, APHA, 1989).

4.5. Sampling Regime

To investigate membrane performance for a range of solids concentrations, it was sometimes necessary to concentrate the influent sludge. During these runs, the sludge composition in the feed tank was therefore different to that of the crude feed sludge.

Samples were taken from four points on the rig:

1. Crude sludge, directly from the BNR plant and sampled prior to the strainer
2. Concentrated sludge, well mixed sludge taken from within the feed tank
3. Permeate stream 1, the permeate taken from the sample point on permeate stream 1
4. Permeate stream 2, the permeate taken from the sample point on permeate stream 2

A suite of samples were taken once during each run (normally 24 hour duration), and analysed for the following:

- SS
- BOD_5
- COD
- NH_3-N
- Total Kjeldahl N
- DOC

These samples were sent for analysis at Whitlingham laboratory. The analyses were performed according to the HMSO blue book methods (1979,1980,1981,1986,1987).

Supplementary analysis included:

- SS concentration of feed tank during concentration. Performed according to Section 2-75, APHA, 1989.
- Tubidity, using a 'HACH 2100P' turbidimeter. Nephelometric method, Section 2-13, APHA, 1989.
- Temperature of sludge, using a 'Whatman Thermopen' thermometer.

4.6. Method used to investigate the effect of changing permeate back pressure

To accurately measure the effect of changing pressure, a manometer was set up on the permeate line. The routing of the permeate outlet was then altered to increase or reduce the pressure. The arrangement is shown in Figure 4.5:

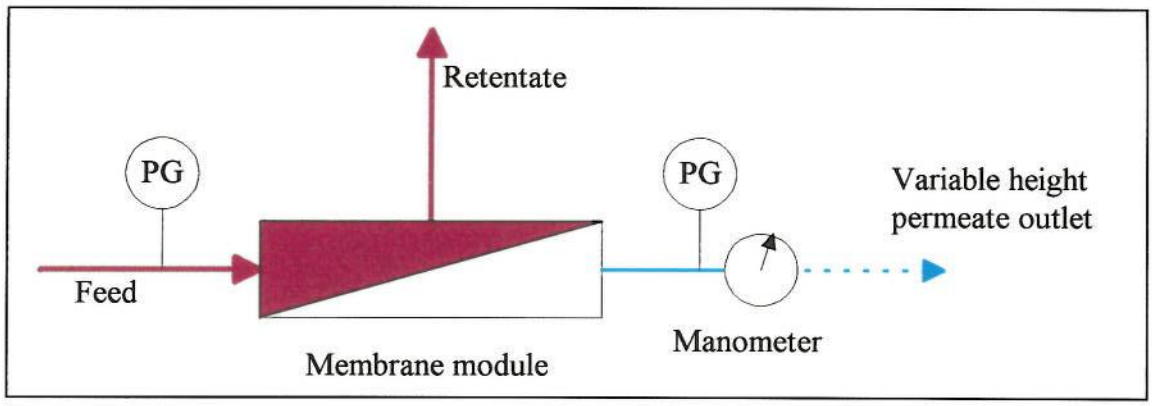

Figure 4.5 Experimental apparatus for investigating flux dependency on permeate line pressure

4.7. Sources of experimental error

As with all practical experiments, there are many sources that can contribute to the error. Some sources of experimental error present during these trials are listed below:

- Temperature change
- Sample analysis inconsistencies
- Instrument calibration
- Differences in sludge composition

This non exhaustive list shows some factors which can cause inconsistencies and errors in the results.

5. RESULTS

5.1. Clean water flux

In the absence of fouling, the relationship between flux and trans-membrane pressure is linear according to equation [2.1]. Before the wastewater experiments were started, the feed reservoir was filled with tap water. The flux was measured for increasing trans-membrane pressure, with the results shown in Figure 5.1.

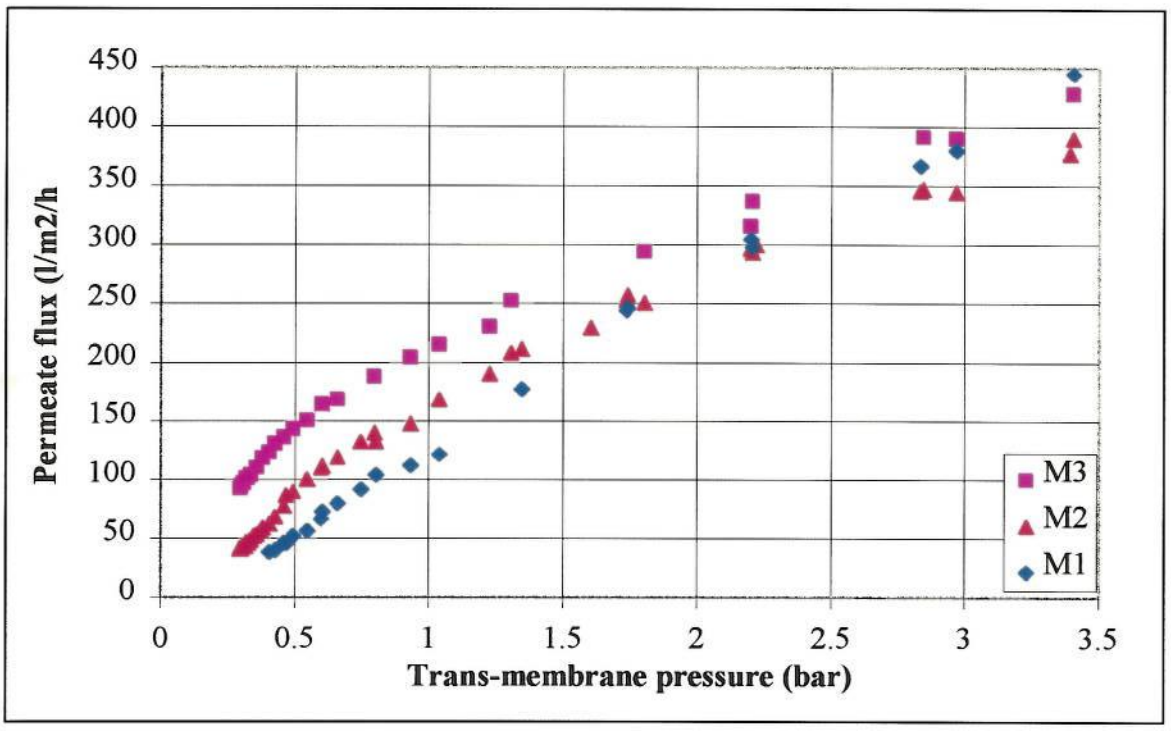

Figure 5.1 Clean water flux-pressure relationship with cross flow velocity = 3.1 ms^{-1}.

Initially, the relationship is approximately linear, with a changing gradient above around 1 bar. The graph shows that the flux per unit pressure varies between modules, particularly up to around 2 bar.

5.2. Flux decline due to fouling

With the feed reservoir supplied with sludge from an external source, experiments to determine the fouling characteristics of the membranes could be performed. Preliminary studies showed that flux decline was greatest in the first few hours of filtration, with a gradual stabilisation of the flux produced. Figure 5.2 shows an example of the flux decline for the three membranes over a 24 hour period.

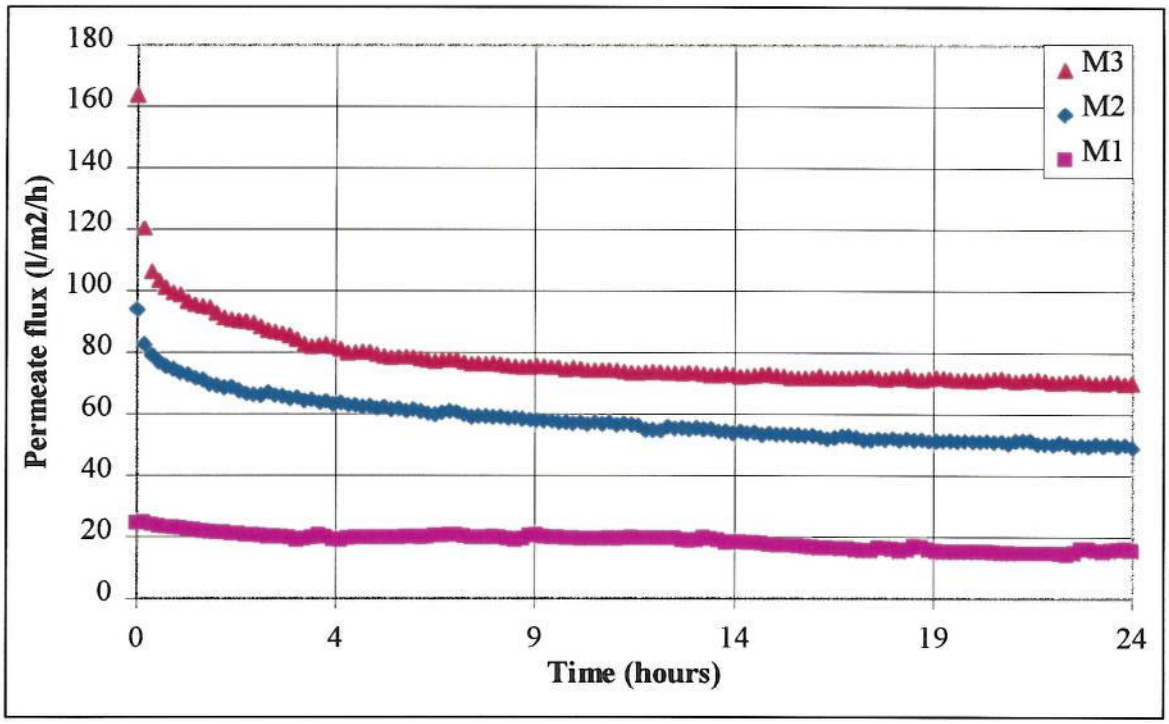

Figure 5.2 Flux decline over 24 hours. Feed SS concentration = 2,500 mgl^{-1}, cross flow velocity = 3.1 ms^{-1}.

The flux after 24 hours was the point chosen for assessing the extent of fouling, as after this period of time the fouling behaviour appears well established.

5.3. Variables used during trials

The flux after 24 hours was used when comparing membranes under differing operating conditions. The variables used in the comparison can be summarised as shown in Table 5.1:

Table 5.1 Variables used during comparative investigation

Variables		
Membrane type	Cross flow velocity (ms^{-1})	Feed solution SS concentration (mgl^{-1})
M1	2.3	2,500
M2	3.1	5,000
M3	3.9	7,500

5.3.1. Hydrodynamics:

The Reynolds number, Re for these conditions must take the solution characteristics into account. As the suspended solids concentration is high, both the density and viscosity will be affected as described in Section 2.6.3.

For these tubular membranes, the characteristic dimension, d, is the diameter of the tubes. Therefore d = 12mm.

The values of Re during the trials can therefore be summarised in the Table below:

Table 5.2 Re under the operating conditions used

Velocity (ms^{-1})	SS (mgl^{-1})			
	2,500	**5,000**	**7,500**	**15,000**
2.3	21,600	17,600	14,400	7,880
3.1	29,100	23,800	19,400	10,600
3.9	36,600	29,900	24,400	13,400

5.4. Comparison of flux produced

5.4.1. Permeate flux:

The permeate flow rate is used to calculate the permeate flux using the following relationship:

Permeate flux ($l/m^2/h$) = Flow ($lmin^{-1}$) * 60 (min/hour) / membrane area (m^2)

The permeate flow rate ($lmin^{-1}$) and trans-membrane pressure (bar) were recorded for each run. The trans-membrane pressure is dependant on the feed flow velocity and the fouling present.

5.4.2. Specific flux:

Figure 5.3 shows a typical relationship between final flux, specific flux, cross flow velocity and ΔP. The graph shows that the final ΔP does not follow a linear increase with velocity. The same observation is true with the permeate flux. These two effects cause the specific flux to reach a maximum at a cross flow velocity of 3.1 ms^{-1}.

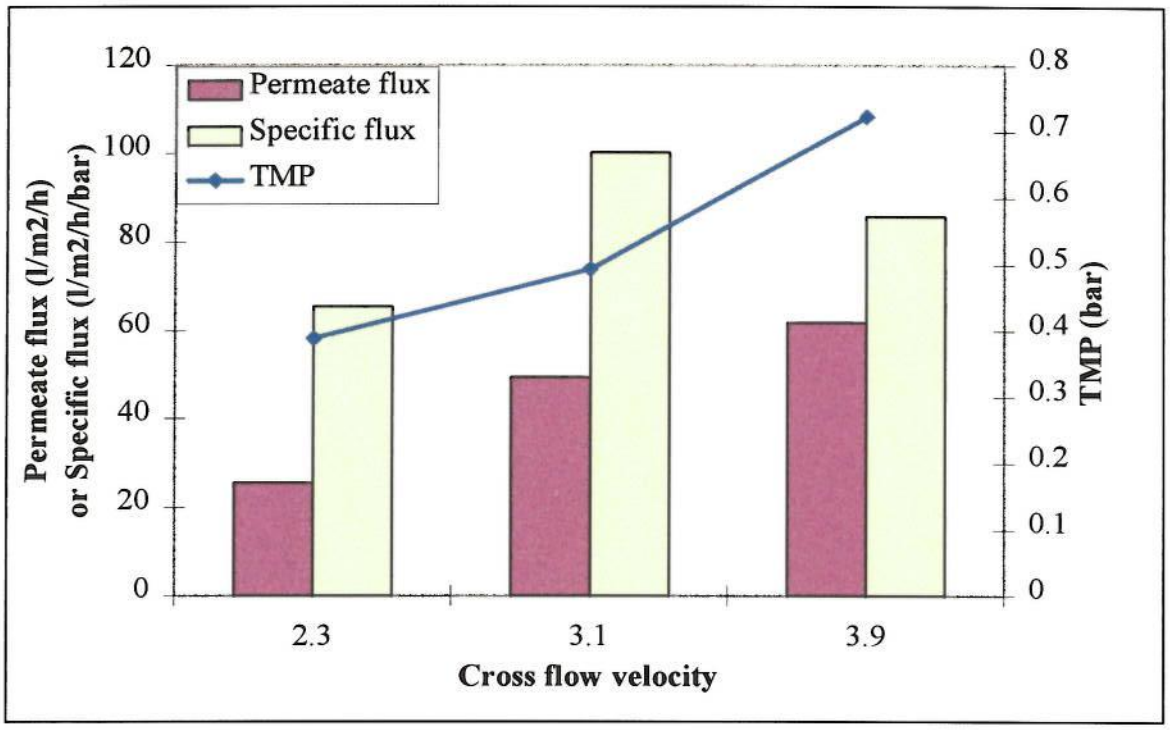

Figure 5.3 Inter-relationship between permeate flux, ΔP, velocity and specific flux. Performed on M2 module at a SS concentration of 2,500 mgl^{-1}.

To allow direct comparisons to be made, the data has been normalised with respect to trans-membrane pressure. This is achieved using the following relationship:

Specific flux, $J_{specific}$ ($lm^{-2}h^{-1}bar^{-1}$) = flux per unit pressure

$$= \frac{\text{Flow } (lmin^{-1}) * 60}{\text{membrane area } (m^2) * \Delta P \text{ (bar)}}$$

5.4.3. Individual membrane performance:

The results shown in Figures 5.4 to 5.6 below show the specific flux after 24 hours continuous operation. The graphs show the performance of each membrane module at three cross flow velocities and SS concentrations. The x axis error bars show the standard deviation of the solution concentration measurements. The R^2 values show the correlation of the points with the trend lines.

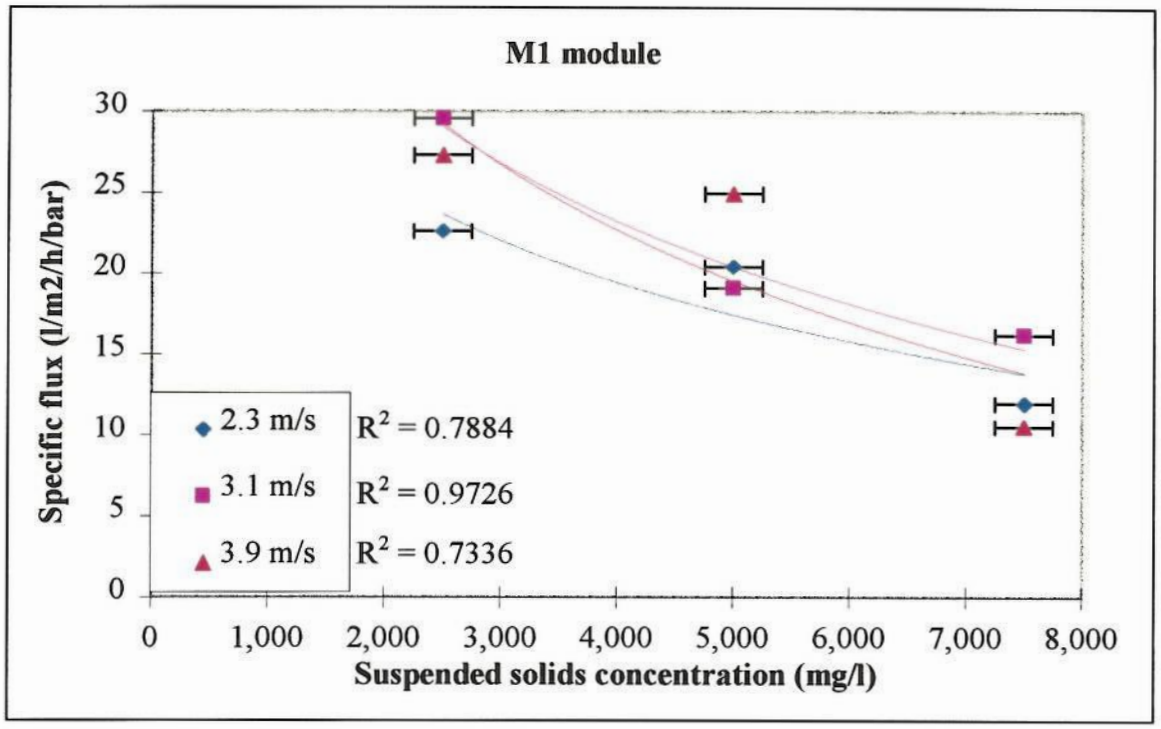

Figure 5.4 Final flux from M1 module for increasing SS concentration and different cross flow velocities

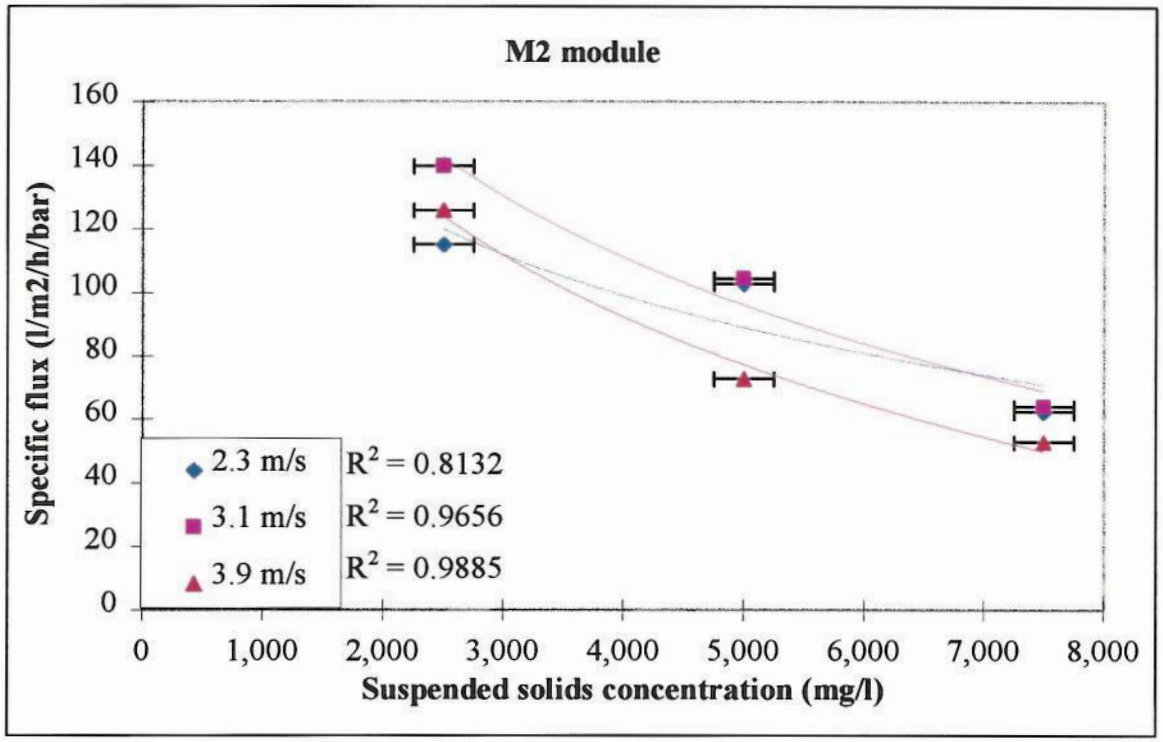

Figure 5.5 Final flux from M2 module for increasing SS concentration and different cross flow velocities

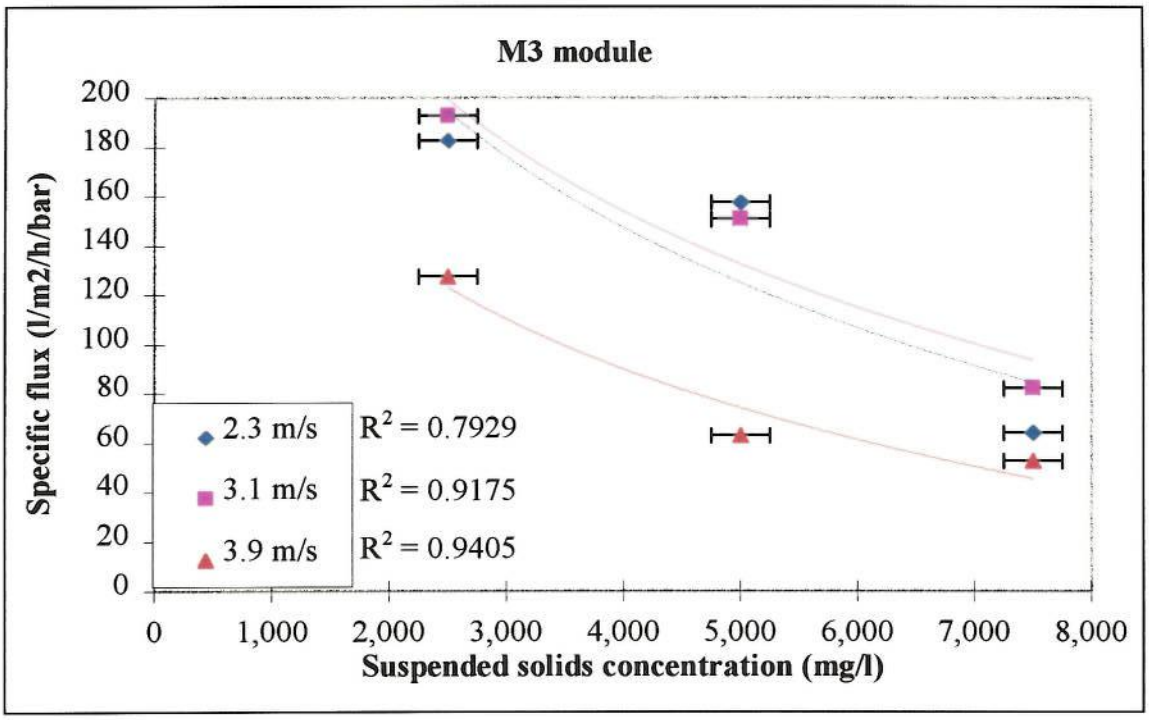

Figure 5.6 Final flux from M3 module for increasing SS concentration and different cross flow velocities

The graphs show a decline in final flux for increasing solids concentration in the feed solution. The results also show that the in general, the maximum specific flux is obtained at a cross flow velocity of 3.1 ms^{-1}. This effect is seen with all three membrane types.

The R^2 values show that in most cases there is a good correlation between the data and the trend lines.

The magnitude of the reduction in final specific flux with the increase in MLSS from 2,500 to 7,500 mgl^{-1} is summarised in Table 5.3 below:

Table 5.3 Effect of increasing MLSS from 2,500 to 7,500 mgl^{-1} on final specific flux

	Reduction in final specific flux, %		
Cross flow velocity, ms^{-1}	M1	M2	M3
2.3	41	41	57
3.1	47	51	53
3.9	53	59	63

Table 5.3 shows that the final specific flux shows a higher reduction at a cross flow velocity of 3.9 ms^{-1}.

5.5. Comparison of membrane performance

The specific flux produced by the different membrane types at different feed concentrations has been compared and the results are shown in Figure 5.7 below. The results are obtained using a cross flow velocity of 3.1 ms^{-1}.

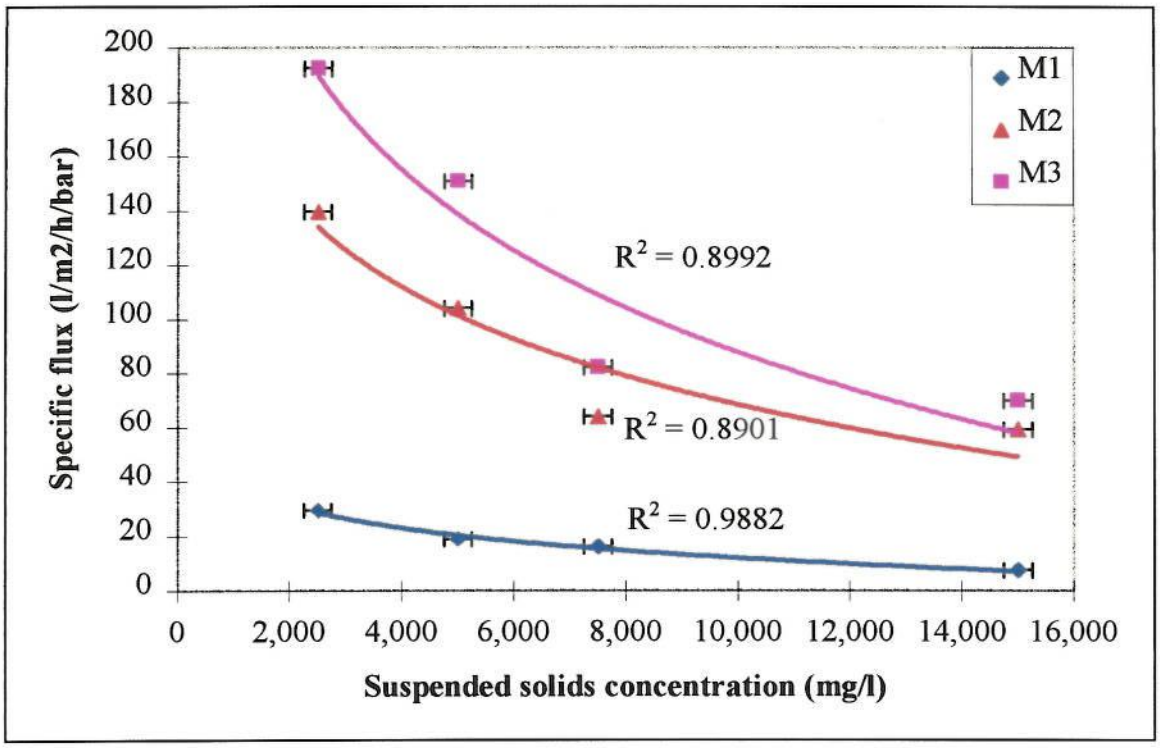

Figure 5.7 Comparison of final specific flux against MLSS at a cross flow velocity of 3.1 ms^{-1}

From this direct comparison under the same conditions, it appears that the permeate flux produced varies widely between module types. The R^2 values show that there is a good correlation between the data and the trend lines. The equations describing the trend lines are detailed in Table 5.4:

Table 5.4 Equations of trend lines for flux-SS relationships

Membrane module	Equation of trend line
M1	J = -12.0 ln (SS) + 123
M2	J = -47.4 ln (SS) + 505
M3	J = -73.4 ln (SS) + 763

With SS in mgl^{-1}

Using these trend line equations, it is possible to estimate the specific flux produced after 24 hours of operation for any MLSS concentration.

5.5.1. Sources of error:

Section 4.7 indicates some possible sources of experimental error which may cause the scatter seen in the previous Figures. Some of the R^2 values are not as close to unity as would be desirable, and the trend lines may not represent the data as accurately as is possible. However, the general flux decline with increasing SS concentration is clear. The difference in performance between membrane modules is also clear, and perhaps more important than the precise flux decline relationship.

5.6. Operating power consumption

The difference in performance seen in Section 5.2 has a strong bearing on the operating costs of the membrane filtration process. As described in Section 2.5, a useful measure of the cost of the process is the energy required to produce the permeate in $kWhm^{-3}$ product water.

The power used during filtration was estimated from the feed flow rate and the pressure drop through the system, as described by equation [4.1]. An assumption was made that the pumps were 70% efficient.

A comparison of the energy consumption after 24 hours continuous filtration for different membranes under different conditions is shown in Figure 5.8 below:

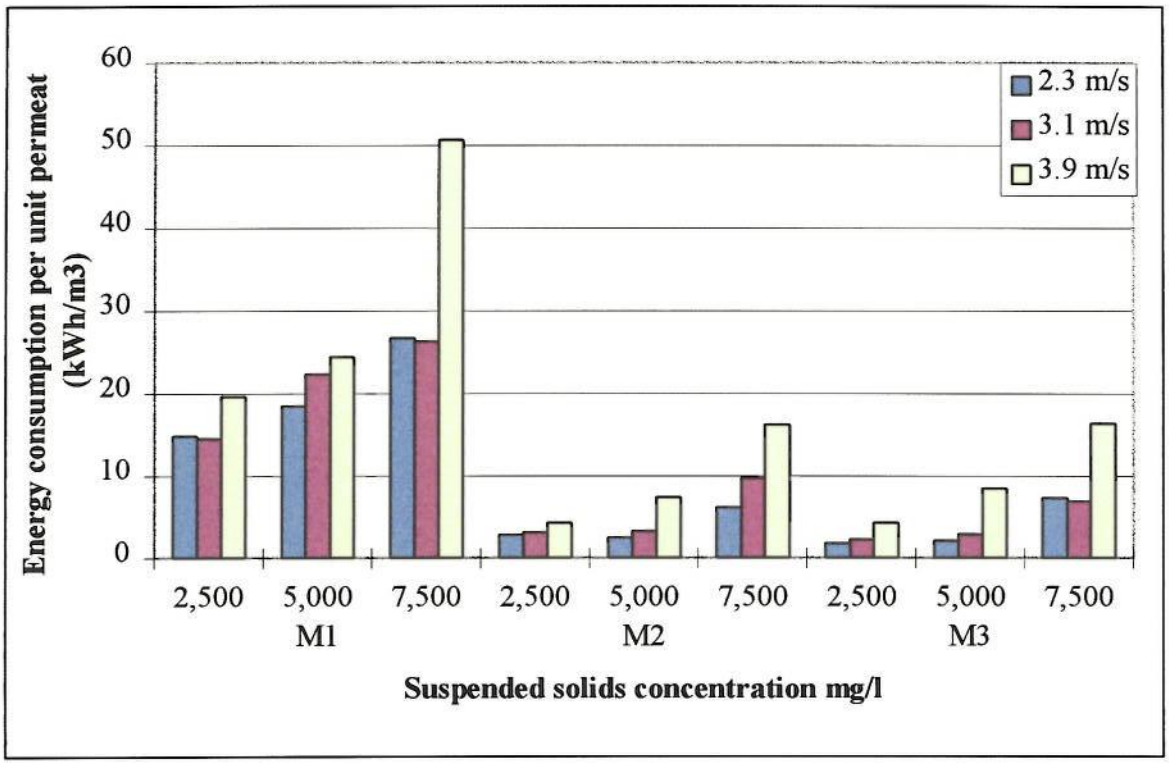

Figure 5.8 Graph showing how energy consumption varies with the operating conditions used

The lower flux produced by M1 has a direct effect on the energy required. This being substantially higher than the other membranes investigated.

The lowest power requirement was achieved by the M3 module, with a value of 1.75 $kWhm^{-3}$. This run was performed at a cross flow velocity of 2.3 ms^{-1} and SS concentration of 2,500 mgl^{-1}.

5.7. Results of sample analysis

The filtration efficiency of the membranes can be assessed by the results of the sample analysis which was performed. A full record of the results of the sample analysis is detailed in Appendix B. A summary of the results showing permeate quality compared with the feed sludge is shown in Tables 5.5 - 5.8. The mean values are given together with the standard deviation of the samples:

Table 5.5 Sample analysis results during 2,500 mgl^{-1} runs

Measurand (mgl^{-1})	Feed sludge in reservoir	M1 permeate	M2 permeate	M3 permeate
SS	2500 ± 207	2.8 ± 1	3.6 ± 1.0	3 ± 2
BOD	1560 ± 324	< 2	< 2	< 2
COD	2960 ± 401	24 ± 5	16 ± 1	25 ± 7
NH_3-N	6 ± 4	0.4 ± 0.3	0.4 ± 0.3	0.3 ± 0.2
TKN	12 ± 6	3 ± 1	2 ± 1	1.8 ± 0.4
DOC	7.2 ± 0.6	6.8 ± 1.4	5 ± 0.3	6 ± 1

Table 5.6 Sample analysis results during 5,000 mgl^{-1} runs

Measurand (mgl^{-1})	Feed sludge in reservoir	M1 permeate	M2 permeate	M3 permeate
SS	4680 ± 295	2.6 ± 1.1	2.6 ± 1.2	< 2
BOD	1900 ± 574	2.3 ± 0.8	< 2	< 2
COD	4700 ± 907	27 ± 7	18 ± 3	21 ± 1
NH_3-N	8 ± 4	3.2 ± 1.1	4 ± 1	2.9 ± 0.8
TKN	215 ± 106	3.6 ± 1.8	3.6 ± 1.4	2.7 ± 0.6
DOC	17 ± 14	8.3 ± 1.9	7 ± 1	6.7 ± 0.5

Table 5.7 Sample analysis results during 7,500 mgl^{-1} runs

Measurand (mgl^{-1})	Feed sludge in reservoir	M1 permeate	M2 permeate	M3 permeate
SS	7230 ± 228	2 ± 0.3	< 2	5.2 ± 4.5
BOD	2810 ± 536	< 2	< 2	< 2
COD	7570 ± 1000	22 ± 7	18 ± 3	30 ± 13
NH_3-N	15 ± 5	0.6 ± 0.5	0.2 ± 0.2	1 ± 0.4
TKN	82 ± 17	3.5 ± 2.2	1.3 ± 0.1	2 ± 0.2
DOC	20 ± 10	7 ± 1	5.5 ± 0.5	6 ± 2

Table 5.8 Sample analysis results during 15,000 mgl^{-1} runs

Measurand (mgl^{-1})	Feed sludge in reservoir	M1 permeate	M2 permeate	M3 permeate
SS	14900 ± 919	5.4 ± 3.7	2.4	< 2
BOD	2960 ± 295	4.8 ± 2.8	4.6	2.1
COD	15600 ± 912	37 ± 4	54.7	26.1
NH_3-N	21 ± 5	6.5 ± 1.0	7.2	5.7
TKN	172 ± 13	5.4 ± 3.7	6.1	< 1
DOC	15 ± 6	10 ± 2	12.2	8.9

Tables 5.4 - 5.7 show that the suspended solids were very low for most samples, giving a very high reduction in the major contaminants of sludge. The reduction in DOC shows that the membranes are rejecting a portion of the macromolecules in solution.

Supplementary analysis performed during each run is detailed in Table 5.8 below:

Table 5.9 Results of supplementary analysis

Measurand	Average ± SD
Temperature of sludge in feed tank (^{0}C)	21.2 ± 0.75
Turbidity of permeate from M1 (NTU)	0.26 ± 0.11
Turbidity of permeate from M2 (NTU)	0.16 ± 0.09
Turbidity of permeate from M3 (NTU)	0.14 ± 0.05

5.8. Investigation into sub-critical flux operation

The rig was operated with a low ΔP for extended periods of up to 42 hours. The permeate flux was limited with a valve, which also served to reduce ΔP. An example of the results of these trials is shown in Figure 5.9:

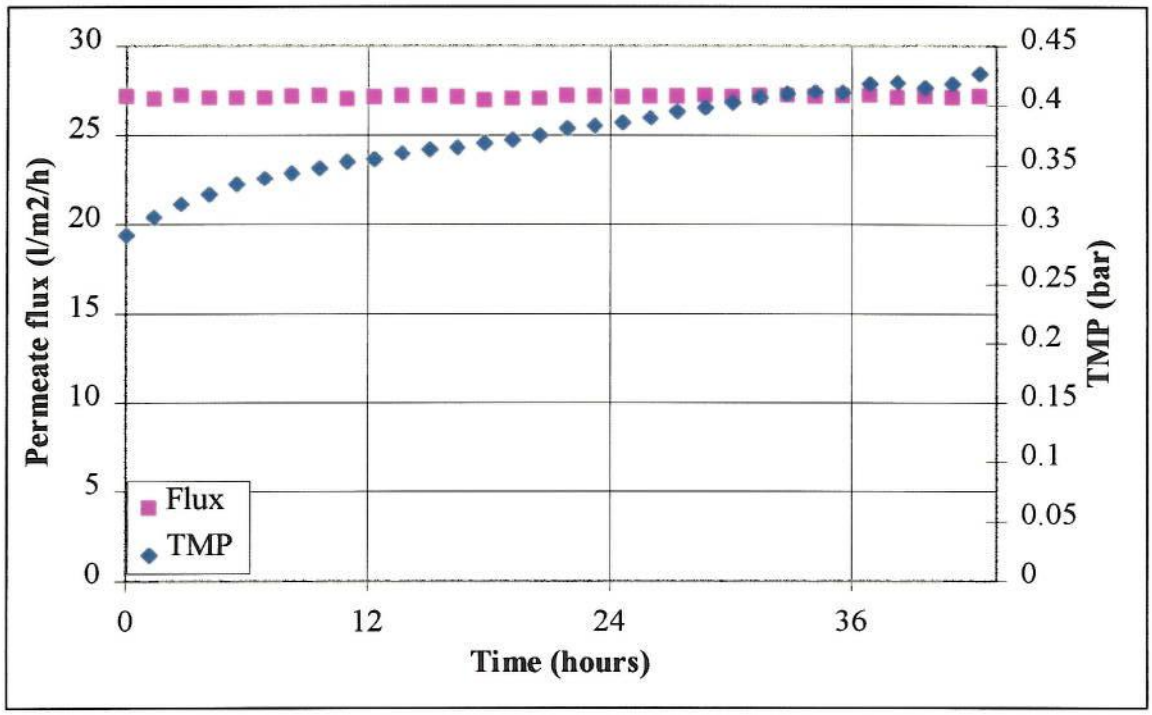

Figure 5.9 Operation at low ΔP in an attempt to find dynamic balance. SS = 2,500 mgl^{-1}, cross flow velocity = 2.3 ms^{-1}

As Figure 5.9 shows, ΔP increases throughout the run. This indicates that the system has not found a dynamic balance, and that fouling will continue to increase the ΔP with time.

5.9. Increasing turbulence through periodic high velocity flow

The ability of periodically high flow rate 'flushes' to reduce the cake layer deposits on the surface of the membrane has been investigated.

The runs were performed using sludge with a SS concentration of approximately 2,500 mgl^{-1}. The normal cross flow velocity was 3.1 ms^{-1}, with a flush flow rate corresponding to a cross flow velocity of 3.5 ms^{-1}. The periodicity of the high flow flushes was 60 minutes, and the duration was two minutes. An example run is shown in Figure 5.6 below, where the decline in specific flux is compared with a constant flow rate run:

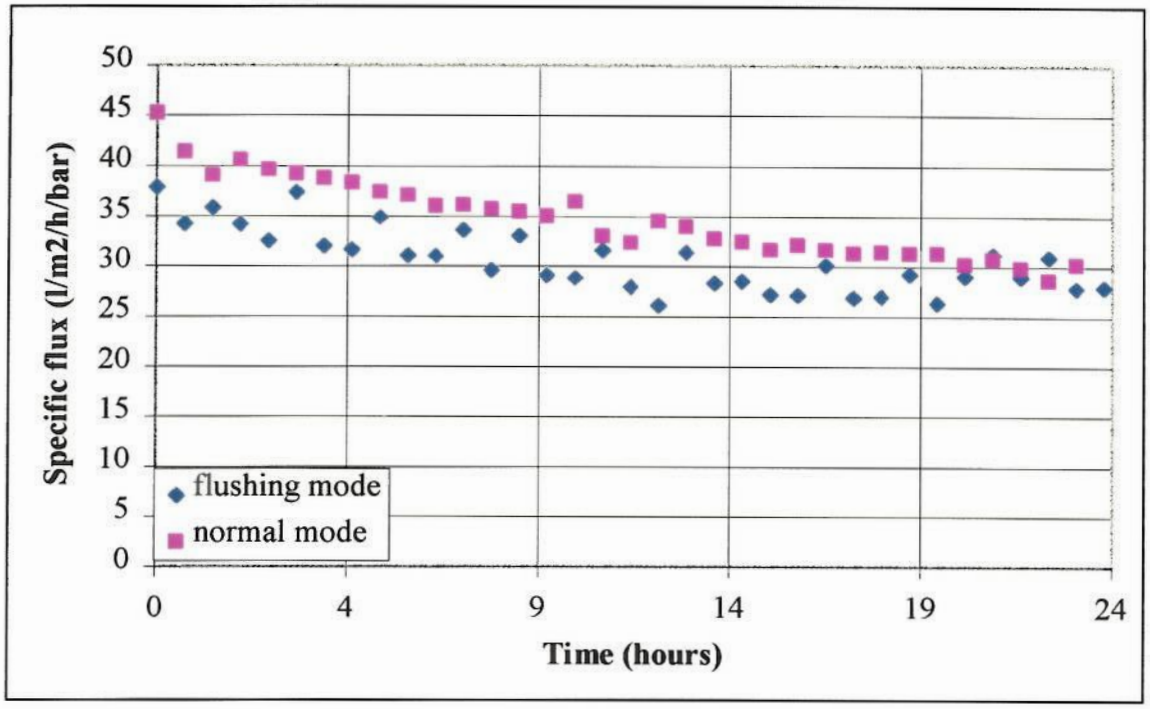

Figure 5.10 Permeate flux during periodic high flow rate flushes, compared with normal declining flux

The flux decline over 24 hours appears to follow the same trend for both operating regimes. However, fractional flux decline from start to end is lower under the flushing regime. For the normal constant flow run, the decline in specific flux after 24 hours = 33%. The decline for the flushing run over the same period = 27%.

5.10. Effect of permeate line pressure on flux

To complete the range of experiments needed to compare flux at different concentrations, the permeate flowed through different pipe-work. This was necessary to maintain the feed reservoir at a concentration different to that of the crude sludge.

As shown in Figures 4.2 and 4.3, there are two possible routes for the permeate to flow. One set of pipes returns the permeate to the feed tank, while another can be used if the permeate is to be wasted to drain. To return the permeate to the feed tank, the pipe-work is routed up over the side of the tank. This increase in height means that when the pipe is flooded, the column of water provides a back pressure.

During operation of the rig, it became clear that any pressure applied to the permeate line caused a decrease in flux. When the permeate routing was changed while filtration was in progress, the permeate flux would change markedly.

An experiment was conducted using the set up shown in Figure 4.5. Using sludge at a SS concentration of approximately 2,500 mgl^{-1} and a range of cross flow velocities, the permeate flux was measured as the permeate line back pressure was varied. The measured TMP was also recorded. The experiments were conducted after 24 hours constant filtration so that flux decline due to fouling during the experiment was minimised. The results are shown in Figure 5.11:

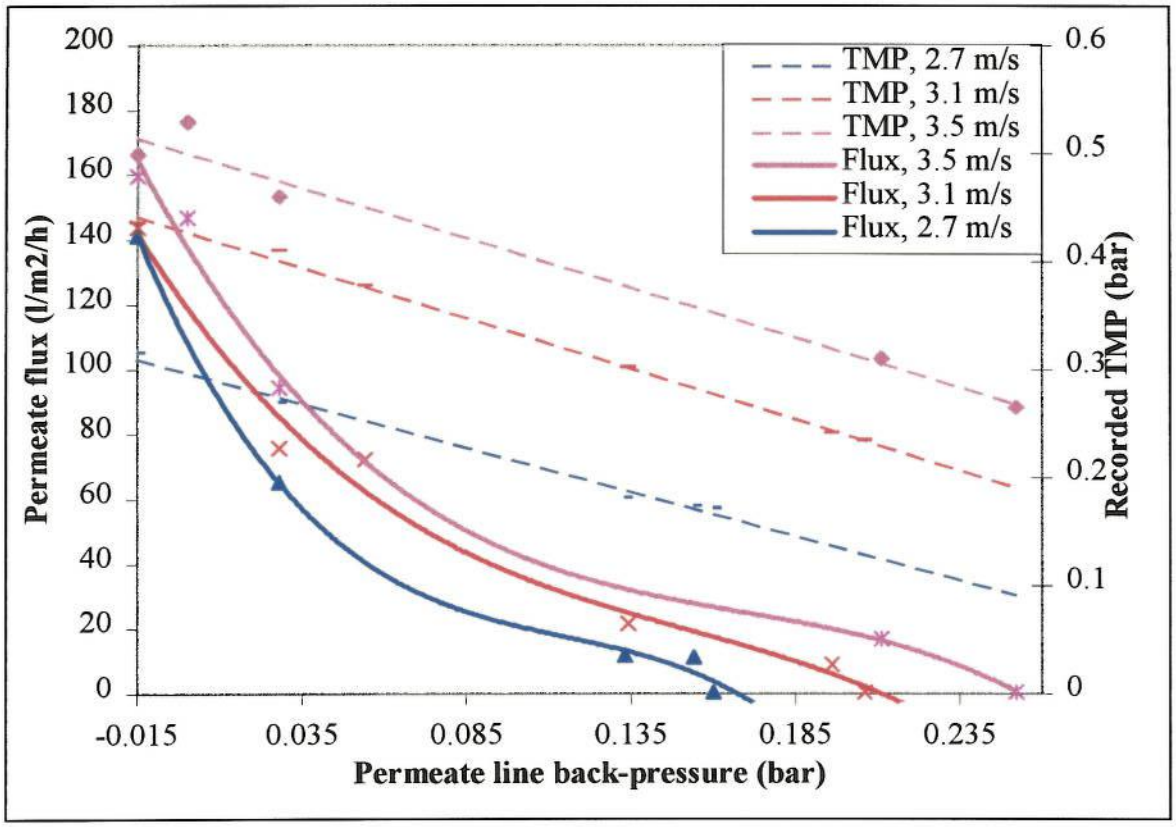

Figure 5.11 Permeate flux against permeate line pressure

These results were taken under the same conditions, with any variation in the solution composition small.

5.10.1. Flux response:

The permeate flux produced over this range of ΔP should be predicted by equation [2.10], where J is directly proportional to ΔP for constant viscosity and total resistance. The change in gradient of the permeate flux lines is not expected, and indicates that there may be a more complex relationship between J and ΔP.

5.10.2. Trans-membrane pressure:

The trans-membrane pressure, ΔP, decreases in proportion to the pressure applied to the permeate line. This is expected as the ΔP is calculated as the pressure difference between the retentate and permeate sides of the membrane.

The fact that the permeate flux becomes zero while a ΔP is still recorded is not predicted by equation [2.10]. The permeate line pressure required to stop the flux is a portion of the measured ΔP, therefore only part of the measured ΔP is driving the flux. The residual pressure recorded is that lost due to friction in the pipe-work and membrane module itself.

5.10.2.1.Frictional losses in pipe-work and membrane module

During the trials detailed above, the SS concentration was approximately 2,500 mgl^{-1}. At this concentration, the dilute sludge can be considered a "Newtonian" fluid. This means that the pressure drop is proportional to velocity and viscosity under laminar flow conditions.

At higher concentrations (> 3% by weight), sludge ceases to behave as a Newtonian fluid, and pressure drop under laminar conditions is no longer proportional to flow - so the viscosity is not constant. Concentrated sludge shows similar behaviour to a Bingham plastic, with a straight-line relationship between shear stress and flow. A method of calculating pressure drop under these conditions is detailed in Metcalf and Eddy (1991).

As the dilute sludge shows similar behaviour to water, the headloss through the system can calculated using the standard methods employed for water.

Loss through a length of pipe is calculated using the Darcy-Weisbach equation, where headloss can be found from:

$$h = f * \frac{L}{d} * \frac{\upsilon^2}{2.g} \qquad [5.1]$$

where
h = headloss in meters of water
f = friction factor
L = length of pipe, m
d = diameter of pipe, m
υ = fluid velocity, ms^{-1}

The friction factor, f, is found from a plot of the Colebrook-White equation (Moody diagram, Perry and Green, 1984). To use this plot, a value for the relative roughness must be found. This is the ratio of roughness to pipe diameter. The roughness used corresponds to the material of the pipe itself. The roughness value, k, used was 0.0025 mm. Together with the Reynolds numbers calculated in Section 5.3.1, a friction factor of 0.025 was indicated.

Losses due to bends and obstructions in the pipe-work can be calculated using the k value system. Values for different k values are shown in Appendix C. The headloss is calculated from:

$$\delta h = k * \frac{\upsilon^2}{2.g} \qquad [5.2]$$

Losses between the feed side pressure gauge and the membrane module have been calculated for a range of flow velocities.

At the point of zero flux, the permeate pressure will be equal to the average pressure on the retentate side of the membrane. Therefore, the total pressure drop due to friction can be calculated.

The total headloss at a range of fluid velocities is shown in Figure 5.12 below. Also shown on the same scale, is the difference between recorded ΔP and the back-pressure required to stop permeate flux.

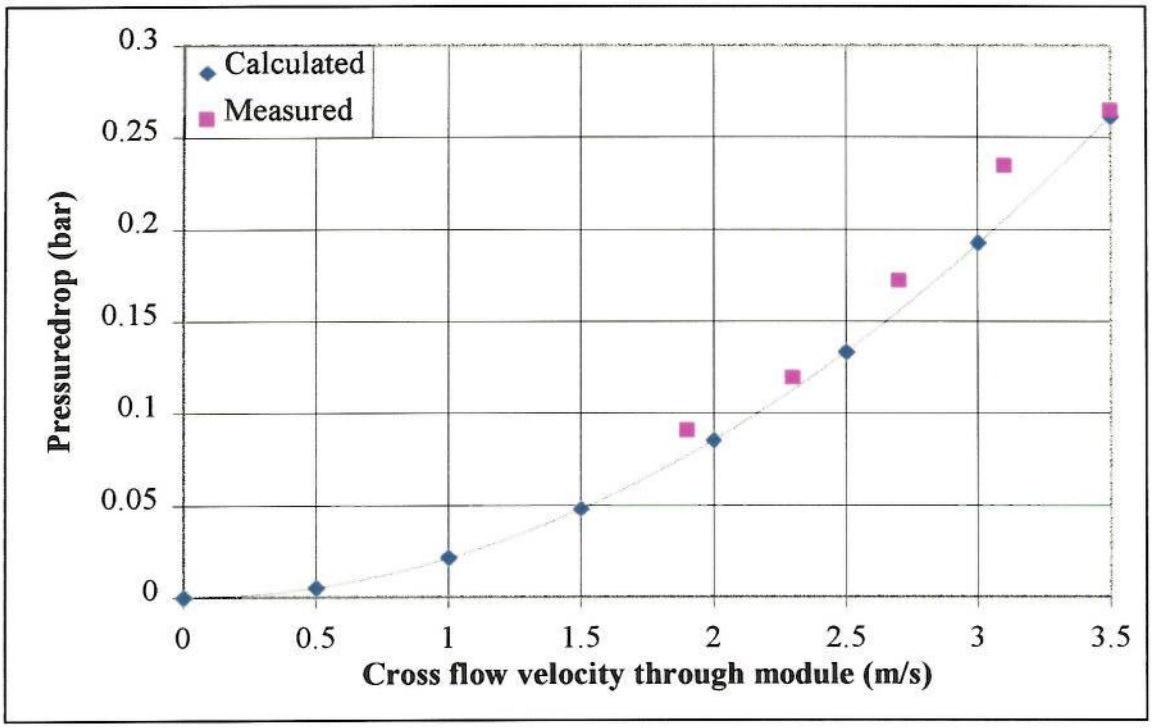

Figure 5.12 Calculated headloss and measured pressure loss at different cross flow velocities.

These data sets appear to follow a close relationship, and it is likely that this gives an accurate picture of the pressure losses incurred through this type of module.

6. DISCUSSION

6.1. Clean water flux

The results of the clean water runs (Figure 5.1) show an approximately linear relationship between permeate flux and trans-membrane pressure at low pressures. This is as predicted by equation [2.1] under conditions of constant viscosity and membrane resistance. The relationship deviates from the linear above approximately 1 bar gauge. This is probably due to the formation of a fouling layer. Tap water was used, which, together with debris present in the pipe-work, is likely to increase membrane resistance with time.

Using equation [1.1], the resistance of the clean membranes can be calculated and compared.

For this purpose, the permeate flux is converted from $l/m^2/h$ to $m^3/m^2/s$. using the conversion:

$$1\ lm^{-2}h^{-1} = 1/3{,}600{,}000\ m^3m^{-2}s^{-1}$$

And pressure in bar is converted to pressure in Nm^{-2} using:

$$1\ bar = 100{,}000\ Nm^{-2}$$

For this calculation, only the flux measurements up to 1 bar are used, to avoid inaccuracies due to the influence of fouling. Figure 6.1 shows the results, together with the best fit lines whose equation is used in the calculation:

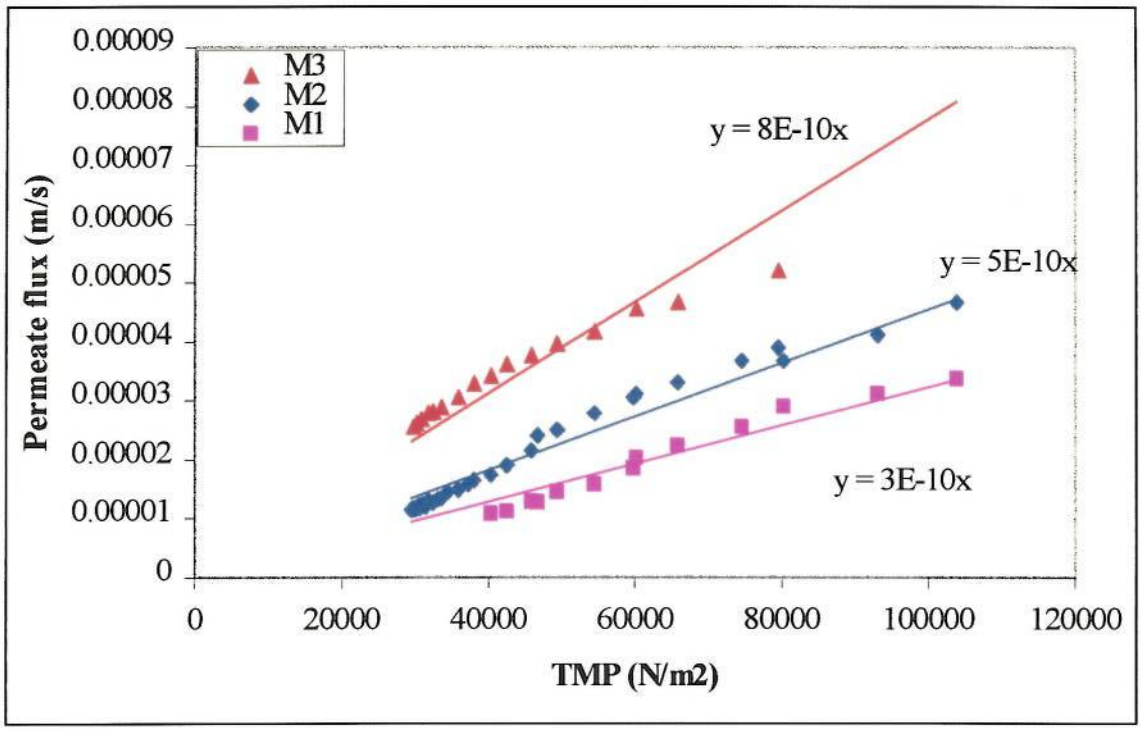

Figure 6.1 Permeate flux - pressure relationship

Using the best fit line equations, and a rearranged version of equation [2.1], the resistance of the membrane can be estimated:

$R_M = \Delta P / J \,.\, \mu$

where $\Delta P / J$ = 1 / gradient of line in Figure 6.1.
μ = viscosity of water = $1.01*10^{-3}$ Nsm^{-2} @ 20^0C

The values calculated are shown in Table 6.1:

Table 6.1 Resistance of the membranes to clean water

Membrane	$\Delta P / J$	R_M (m^{-1})
M1	$3.33 * 10^9$	$3.30 * 10^{12}$
M2	$2.00 * 10^9$	$1.98 * 10^{12}$
M3	$1.25 * 10^9$	$1.24 * 10^{12}$

Magara and Itoh (1991) found values of approximately $1*10^{13}$ m^{-1} for the membrane resistance to the passage of clean water. This is higher than any of the resistances shown above. However, the membranes used in their trials had a MWCO of between 20,000 and 50,000 Da. The lower average pore size may explain the higher resistance to clean water than those found in this study.

6.2. Filtration of wastewater

The membrane filtration of wastewater is subject to fouling by the contaminants present, both particulate and dissolved matter. The range of conditions used during these trials gives a good indication of how the membranes will behave when used for solid-liquid separation in an MBR.

6.2.1. Flow regime during trials:

The increased physical scouring and back diffusion at the membrane surface generated during turbulent flow is thought to reduce the build up of fouling. The flow regime for fluid flow through a pipe is normally considered turbulent if the Reynolds number > 4000. As the feed solution contained a high concentration of suspended solids, the density and viscosity are greater than for clean water.

To take these factors into account, the empirical relationships developed by Krauth and Staab (1993) have been used. Table 5.2 shows the modified Reynolds numbers for the operating conditions used during these trials. According to this correlation, the flow is turbulent during all conditions encountered, with a minimum Re of 7,880 at the highest solids concentration and lowest velocity. This means that changes seen in flux production cannot be attributed to a change between laminar and turbulent flow regimes.

6.3. The effect of cross flow velocity and pressure

6.3.1. Specific flux:

During the filtration of suspensions and solutions, changes to the operating conditions can have a strong effect on the permeate flux. An increase in cross flow velocity has been found to increase the permeate flux by several authors (Al-Malack and Anderson, 1997, Magara and Itoh, 1991 and Krauth and Staab, 1993).

This study has investigated the relationship between cross flow velocity and permeate flux. However, the change in cross flow velocity was gained by altering the feed flow rate through the system. As the flow rate is increased, the feed pressure is increased giving a higher value of ΔP.

Figure 5.3 shows how the permeate flux, ΔP and the specific flux are related (after 24 hours) for different cross flow velocities. The increasing cross flow velocity gives an increase in the flux produced and in ΔP. To enable a direct comparison, the flux produced has been normalised with respect to pressure. The flux per unit pressure (specific flux) can then be compared to cross flow velocity.

It can be seen in Figure 5.3 that the specific flux does not increase consistently with velocity. Rather, it reaches a maximum and begins to decline. This is probably due to the ΔP exceeding ΔP_C, thus the increase in pressure associated with the change in cross flow velocity does not stimulate an increase in the flux according to equation [2.1].

Although it has not been possible to separate the effect of cross flow velocity and ΔP, the results give a useful indication of the behaviour expected in full scale applications. Using the feed flow rate to alter cross flow velocity is an accepted method for industrial applications.

6.3.2. Optimum conditions:

These results show that there is an optimum value of velocity and ΔP (corresponding to an optimum feed flow rate). Either side of this flow rate, the specific flux will be reduced. For the experimental rig used for this study, the optimum feed flow rate of 400 $lmin^{-1}$ corresponds to a cross flow velocity of 3.1 ms^{-1} in the membrane tube and a ΔP between 0.45 and 0.55 bar.

The reduction in final specific flux with increasing SS concentration also follows this pattern. Table 5.3 shows that the largest flux reduction when increasing concentration from 2,500 mgl^{-1} to 7,500 mgl^{-1} occurs at a cross flow velocity of 3.9 ms^{-1}. The ΔP associated with this velocity is between 0.5 - 0.7 bar. At the end of 24 hours continuous operation, ΔP has risen to 0.7 - 1.4 bar.

If these values for ΔP exceed the critical trans-membrane pressure, ΔP_C, This supports the theory (Howell, 1996) that above ΔP_C the flux does not increase with pressure.

This effect agrees with Elmaleh and Abdelmoumni (1997), who found that steady state flux reached a maximum at a driving pressure of around 1 bar gauge. After this maximum, the flux actually dropped away slowly.

6.4. Effect of SS concentration

Figures 5.4 - 5.7 show how each membrane performed under the range of SS concentrations.

A general decline in final flux is seen with increasing SS concentration. This effect has been noted by previous studies (Beaubien *et al.*, 1996 and Magara and Itoh, 1991), details are given in Section 2.3.3.

The results found in this study show that the decline in flux with increasing SS will vary with the conditions under which the system is operated. Figure 5.7 shows a direct comparison between the three membranes used under similar conditions.

Although there is a decline in flux produced with increasing SS, it is not the same for all membranes. Previously published reports giving general empirical relationships between flux and SS oversimplify the process.

The rate of flux decline with increasing SS will depend on many factors including:

- Membrane type
- Nature of solids
- Hydrodynamic operating parameters

The results found in this report show that the performance and response to changes in operation can vary widely between similar modules.

Previous studies on fouling (Bacchin *et al.*, 1995, Wakeman, 1996) show that particulate fouling is a complex process. Influences such as particle size and membrane surface properties will affect the propensity for surface adsorption and cake formation. The filtration of biomass is subject to more complications due to the effect of the extra-cellular matrix, reported by Hodgson *et al.* (1993).

Some previously reported investigations into the relationship between flux and SS have returned different findings. The operating parameters and empirical relationships found are compared together with the results of this study in Table 6.2 below.

Table 6.2 Comparison of reported dependence of flux on SS

Membrane	Velocity ms^{-1}	Pressure bar	Solution type and concentration mgl^{-1}	Relationship seen	Reference
Ceramic tubular 0.2μm	2.0	0.35	anaerobic WW 2,500 - 22,000	linear	Beaubien *et al.*, 1996
Ceramic tubular 300 kDa	3.0	0.5	synthetic WW 2,100 - 15,400	non-linear	Cicek *et al.*, 1998
Polymeric UF 50 kDa	-	0.3	domestic WW 5,000 - 15,000	non-linear	Magara and Itoh, 1991

The results from these published reports have been compiled and plotted together with the results from this study in Figure 6.2:

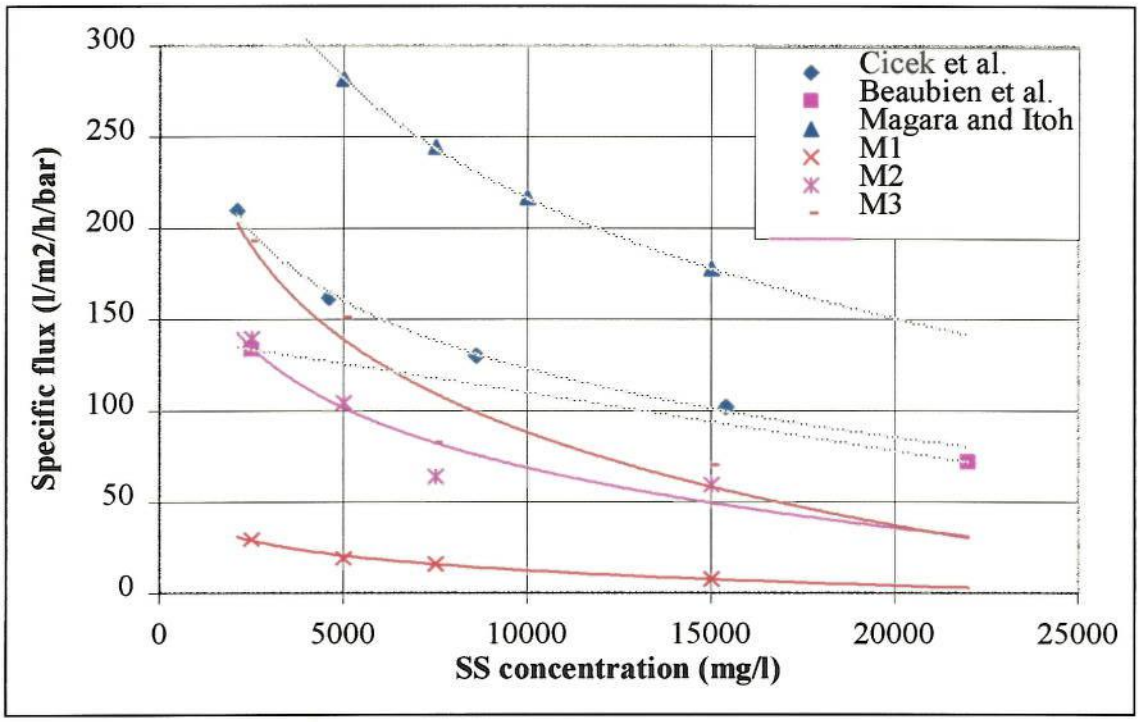

Figure 6.2 Comparison of published trends (Table 6.2) with the authors results at υ=3.1 ms^{-1}, relating specific flux to SS concentration

This comparison illustrates how differences in membrane type and experimental parameters can lead to different responses to changes in SS concentration. The three membranes used in this study were subject to similar conditions, yet their behaviour shows some clear differences.

6.4.1. Estimated maximum SS concentration:

From the trend lines shown in Figure 6.3, it is possible to estimate the SS concentration at which the specific flux tends to zero. By using the equation of the trend line in each case (Table 5.4), and setting the flux to zero, an estimate for the maximum MLSS is obtained. These values are valid for a cross flow velocity of 3.1 ms^{-1} and are shown in Table 6.3 below:

Table 6.3 Estimated maximum SS concentration for the membranes

Membrane	Estimated maximum SS concentration, mgl^{-1}
M1	28,000
M2	42,000
M3	33,000

The specific flux produced by the M1 module is lower than the other two in all circumstances during these trials. The reduction in final specific flux with increasing SS has been shown to be lower in most circumstances (Table 5.3). However, due to low specific flux production at low concentrations, the maximum SS concentration is likely to be lowest.

The M3 module produced a higher specific flux in all the experiments performed. However, from the trend lines shown above, it is clear that the flux is more sensitive to SS concentration. The reduction in final specific flux for increasing SS is greater than for the other modules, with the trend line showing a steeper gradient.

The M2 and M3 modules have an identical specification except for nominal pore size. M3 has a 0.1μm pore size (classed as MF) while the M2 has a MWCO of 250 kDa. The M3 produces a higher specific flux at low SS concentrations (where the membrane resistance is the dominant term in the total fouling resistance) due to the lower resistance as calculated in Section 6.1.

At higher SS concentrations the difference in the specific flux of M2 and M3 is much reduced. This indicates that the filter cake resistance is becoming dominant, and the difference in clean water resistance becomes less significant. The fact that the M3 module is more sensitive to the effects of cake resistance could indicate that it is more prone to pore plugging.

The M2 module has an estimated maximum SS concentration of 42,000 mgl^{-1}. Apart from the incurred error in extrapolating a trend line, the flow regime should also be considered. At a cross flow velocity of 3.1 ms^{-1}, the flow regime will only remain turbulent up to around 27,000 mgl^{-1}. Above this concentration the flow will start to become laminar. This is known to reduce the physical scouring of the membrane surface, and a reduction in the Reynolds number will lower the mass transfer coefficient.

Taking the above points into consideration, it is likely that the limiting SS concentration is lower than that predicted by the trend lines.

6.5. Quantifying the fouling deposits

The resistance in series model was introduced in Section 2.5.2,. This can be used to determine the resistance of the total fouling present, both on the membrane surface and within the structure.

In Section 5.1, the resistance of the membranes to the passage of clean water was determined. With the data gathered during the wastewater filtration, the resistance of the fouling can be estimated as the difference between the membrane resistance, R_M, and the total resistance, R_T.

The method used is similar to that used to calculate the hydraulic resistance. However, in this case the values for the final flux after 24 hrs are used to determine the values of ΔP and J. Although conditions between runs cannot be guaranteed identical, preliminary investigations showed that the flux decline was pseudo-steady after this period of time.

The resistance due to fouling has been calculated for three cross flow velocities (and associated ΔP) at a SS concentration of 2,500 mgl^{-1}. The relationship used is a rearranged version of equation [2.10]:

$$R_T = \Delta P / J \,.\, \mu'$$

and $$R_F = R_T - R_M$$

where R_F = combined resistance of fouling present
μ' = modified viscosity due to solids present (Krauth and Staab, 1993)

The results are shown in Figure 6.3:

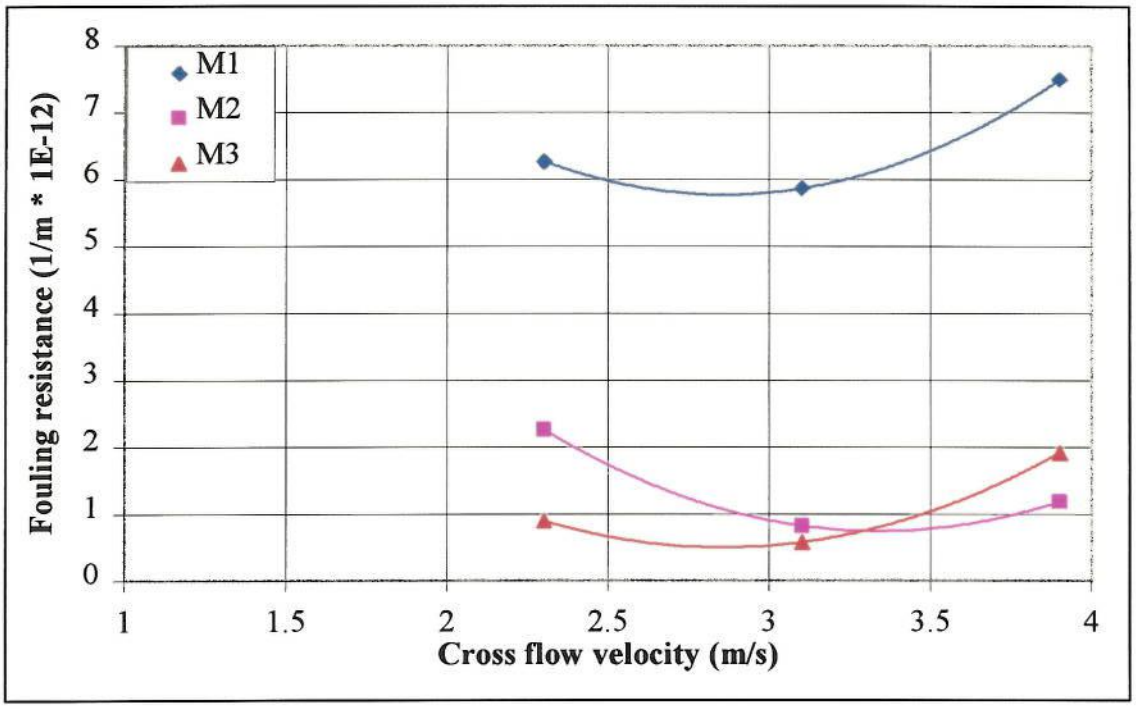

Figure 6.3 Fouling resistance, R_F, change with cross flow velocity at SS = 2,500 mgl^{-1}

These findings show that the resistance of the fouling deposited is dependant on the operating conditions used.

The decline in resistance when increasing velocity from 2.3 to 3.1 ms^{-1} agrees with results found in previous work. Baker *et al.* (1985) found that under conditions of constant pressure the flux increased with velocity. This increase in flux has been attributed to increased shear induced back diffusion.

The increase in resistance above a cross flow of 3.1 ms^{-1} could be due to the combination of two effects:

Baker *et al.* (1985) found that the gradient of the flux-velocity relationship was reduced at higher (> 3 ms^{-1}) velocities. This was attributed to the resistance of the fouling layer becoming less significant than the membrane resistance, and the specific resistance of the fouling layer increasing. This increase in the specific resistance of the fouling layer is thought to result from an average reduction in the size of particles in the fouling layer. This gives a more compact cake and consequently lower porosity.

The increase in cross flow velocity in this study is accompanied by an increase in ΔP. The increased compaction of the cake together with the reduction in the average particle size would lead to a decrease in the porosity and increased likelihood of membrane pore plugging.

These effects are likely to be responsible in the increase in fouling cake resistance at velocities > 3.1 ms^{-1} seen in Figure 6.3. The minimum resistance corresponds to a cross flow velocity of between 2.8 - 3.3 ms^{-1} for all membranes tested. This cross

velocity range and associated ΔP would be the most efficient mode of operation, corresponding to the highest specific flux.

6.6. Likely causes of differences between membranes

From the direct comparisons shown in Figures 5.1, 5.7 & 6.2, clear differences can be seen between the flux produced by different membranes under similar conditions.

The modules are of the same geometry, and the manufacturers data for M1 and M2 is identical in terms of MWCO. The differences in performance between these two membranes could be due to several factors:

- Differences between streams 1 & 2 of the rig

As described in Chapter 4, the experimental rig accommodates 2 membrane modules at a time. As these two separate streams were used to compare the different membranes, it was necessary to ensure that they operated under identical conditions. The modules were mounted in the rig at different heights, and due to the effect of permeate line back-pressure, this meant that conditions were not directly comparable.

To ensure that the comparisons between membranes were valid, the membranes were commutated between stream 1 & 2. The effect on permeate flow due to the height difference was recorded, and the presented results normalised to negate this effect. Hence, differences between stream 1 & 2 can be ruled out as a cause of the difference in performance of the modules.

- Membrane material differences

The only quoted difference between M1 and M2 is the material from which the membrane is fabricated. Magara and Itoh (1991) found that permeate flux can be strongly influenced by the membrane material. Three types of UF membrane were used (polyacrylnitrile, polyolefin and polysulphone) with similar quoted MWCO values. The polysulphone membranes generated the least flux, which was approximately 25% of the flux generated by the highest performing type (polyacrylnitrile).

- Porosity

The membrane resistance to clean water calculated in Section 6.1 shows clear differences between the three modules. The increase in resistance to clean water follows the same order as the decrease in final permeate flux, i.e. the membrane with the highest resistance produces the lowest flux during filtration of suspensions. The M3 module, which has the lowest resistance to clean water, also gives the highest values of final specific flux. As it has the largest pore size, this indicates that the porosity plays an important role in determining the specific flux.

As the resistance due to fouling is of the same order as the clean water resistance (Section 6.3), the clean water resistance has a strong bearing on the flux produced.

6.7. Energy consumption

Figure 5.8 shows the estimated energy consumption for the membrane filtration in terms of power used per unit permeate produced. The power required is a function of the feed flow rate and the pressure drop across the module. The pressure and final flux were recorded at the end of each 24 hr run.

As the pressure drop across the modules is similar when clean, and the same range of flow rates were used, the differences in the results are due to two factors:

- As discussed in Section 6.5, the specific flux produced by each module differed by a large amount.
- The pressure drop across the module at the end of a run will be affected by the degree of fouling accumulation. If a membrane is badly fouled, the increased pressure drop will increase power costs.

The M3 had a lower power consumption in almost all conditions investigated. The two UF modules (M1 and M2) appear similar 'on paper', though there is a substantial difference in performance.

The lowest energy consumption recorded was 1.75 $kWhm^{-3}$ using the M3 module. The results had a large range (1.75 - 50.6 $kWhm^{-3}$) depending on membrane type and operating conditions. The values found in previously published studies are shown in Table 2.9, which shows that the highest value found in previous studies was 27 $kWhm^{-3}$ by Krauth and Staab (1993).

One reason for the high energy consumption found in this study is due to the nature of the experimental rig design. The two streams are each designed to accommodate one membrane module (Section 4.1). These tubular modules operate with a low recovery i.e. the ratio of permeate flow to feed flow is low (0.1 - 1%). The energy required to produce the feed flow rate required is not all lost after the stream has passed through one module, and hence energy is wasted when the stream exits the pipe-work into the feed tank.

When used on full scale plants, the modules are arranged in series and the overall recovery of the array increases accordingly. This would reduce the power consumption required per unit permeate.

At the lowest energy consumption, the filtration power cost per unit permeate is still six times greater than the cost of conventional treatment (as shown in Table 2.9). The advantages gained through the use of an MBR need to be substantial to support this increased cost.

6.8. Permeate water quality

The results of the routine analysis show that the membrane filtration removes a large proportion of the contaminants present in the feed wastewater. The average removal efficiencies are summarised in the table below:

Table 6.4 Average removal efficiencies of the membranes

	Removal, %		
Contaminant	**M1**	**M2**	**M3**
SS	> 99	> 99	> 99
BOD	> 99	> 99	> 99
COD	> 99	> 99	> 99
NH_3-N	60 - 96	50 - 98	63 - 93
TKN	75 - 98	83 - 98	85 - 98
DOC	5 - 65	30 - 72	16 - 70

These removal rates concur with previous reports on MF and UF of biomass solutions, as shown in Table 2.3. It should be noted that the results of analysis for SS and BOD were frequently reported as "< 2 mg/l" when the levels were below the limit of detection. For the statistical analysis these values were included as 2 mg/l. This will have increased the calculated mean value, hence the removal rates quoted in Table 6.3 are conservative.

Although no bacteriological analysis was performed, the rejection of other contaminants is similar to that of Cicek *et al.* (1998). Their study used a similar membrane (UF, 300 kDa MWCO) and found complete rejection of heterotrophic micro-organisms and viruses. As M1 and M2 have a lower quoted value for MWCO, it can be assumed that the rejection of micro-organisms would be similar.

The removal of suspended solids to levels below the limit of detection is commonly reported using MF and UF membranes, as shown in Table 2.3. The conservative figures for solids removal shown above are in good agreement with the published results (Ueda *et al*, 1996, Trouve *et al.*, 1994, Cicek *et al.*, 1998).

A reduction in the dissolved organic carbon content shows that large organic molecules as well as particulate matter are being rejected by the membrane. The retention of high molecular weight compounds is thought to explain the improved mineralisation of organic matter in MBRs (Brindle and Stephenson, 1995).

6.8.1. Comparing membrane types:

The rejection of contaminants is similar with all membranes tested. The M3 membrane has a higher quoted nominal pore size than the M1 and M2 types. This shows that the selectivity of all membranes is similar, yet the benefit of the higher porosity is still received. The M3 module has shown consistently higher specific

fluxes, and proved to have the lowest energy consumption. In the situation simulated with this study, namely a side-stream MBR, the M3 module has shown better performance.

6.9. Sub critical flux

As described in Section 2.7.5, some authors (Howell, 1995 and Field *et al.*, 1995) have reported a stable permeate flux under certain conditions. To maintain a stable flux, it is thought that the trans-membrane pressure, ΔP, should be kept below a certain 'critical pressure', ΔP_C.

Operating the membrane filtration in this way is thought to maintain a dynamic balance between fouling layer build up and removal. In this situation, the ΔP should remain constant once a balance has been established, showing that there is no significant increase in fouling over time.

Several runs were performed, with a stable permeate flux of 27 $lm^{-2}h^{-1}$. The runs were performed on the M3 membrane, at a SS concentration of 2,500 mg/l. As the initial ΔP is determined by the feed flow rate, different rates of feed flow were used.

The example results shown in Figure 5.9 show that the ΔP increased steadily throughout the runs, with no indication that a dynamic balance was occurring.

During previous studies into sub-critical flux operation, Howell (1995) used the conditions shown in Table 6.5:

Table 6.5 Experimental conditions used for sub-critical flux operation (Howell, 1995)

Solution	5% dry weight yeast solution
ΔP	0.1 bar
Module type	0.14 μm pore size, tubular membrane
Turbulence promoter	Helical baffle insert in membrane tube

In all cases where sub-critical flux operation was recorded, a turbulence promoting device was used within the module. The flux enhancing effect of these devices has been reported by several authors (as described in Section 2.7.4.2). It is probable that the use of a baffle has made the sub-critical operation possible at the low velocity which was used. During a similar trial without the baffle fitted, Howell (1995) found that the ΔP increased with time.

During the trials performed in this study, increasing the cross flow velocity will result in a corresponding increase in pressure. It is likely that to provide the turbulence necessary to maintain a dynamic balance, a cross flow velocity would be required which would cause the ΔP to exceed the critical pressure.

Hence, with experimental rig used for these trials, it is likely that sub-critical flux operation would only be possible with some additional source of turbulence or wall shear.

6.10. High flow flushes

The flow regime is known to have a strong influence on the fouling characteristics of a system. Increasing turbulence is thought to increase the physical scouring of the membrane surface and hence reduce the fouling cake layer.

Pulsatile flow has been found to improve stabilised flux (Bertram *et al.*, 1993 and Jaffrin *et al.*, 1987). This method is thought to destabilise the fouling layer and in some circumstances induce a backwashing effect.

Boonthanon *et al.* (1991) also found the use of pressure waves beneficial in improving flux and reducing flux decline. Their method bears similarities with the technique used in this study. The closing off of the permeate line valve (and thus removing convective transport to the membrane surface) is common to both techniques.

The aim of these trials was to investigate the effect of a periodic increase in flow velocity (by raising the feed flow rate), coupled with a temporary removal of mass transfer across the membrane surface (by closing the permeate line valves).

In the experiment reported by Boonthanon *et al*, the permeate line was closed instantaneously using a solenoid valve. The shock wave created by the sudden closing of the permeate solenoid valve was highlighted as a possible cause of fouling layer destabilisation.

The results as shown in Figure 5.10 are inconclusive, as the reduction in flux decline is not significant enough to be outside experimental variation. The use of slow motorised valves to close the permeate line would not have created a significant pressure shock wave. Without this shock wave to destabilise the fouling layer, it is likely that the technique is less effective, which may explain the inconclusive results.

6.11. Effect of permeate line back pressure

The investigation into the effect of permeate line back pressure was undertaken due to inconsistencies in membrane performance noted during the main trials. By carefully examining the effect of small changes in pressure, some useful information has been gathered.

6.11.1. Trans-membrane pressure:

Figure 5.12 shows that the pressure drop across a single membrane is high. Trans-membrane pressure is normally determined by measuring the pressure of the feed

stream and that of the permeate stream. The difference between them is then quoted. This work shows that only a proportion of this quoted value is used to drive the filtration process, the rest lost due to friction through the pipe-work and module.

These results show that the pressure drop through the membrane module must be considered carefully when designing a filtration system.

6.11.2. Non-linear flux response:

Figure 5.11 shows that the flux does not appear to increase in proportion with the increasing ΔP. The shape of the curves showing permeate flux against back pressure applied to the permeate line do not follow the linear relationship predicted by equation [2.10]. With an applied back pressure on the permeate line, initially the flux drops away rapidly, before showing a decline proportional to the decreasing ΔP.

Further measurements were taken to investigate the effect of a small negative pressure on the permeate line. The cross flow velocity for this set of results was 3.5 ms^{-1}, again using a SS concentration of 2,500 mgl^{-1}. The results are shown in Figure 6.4 below, where the corrected TMP indicates that the head loss calculated in Section 5.10.2.1 has been taken into account:

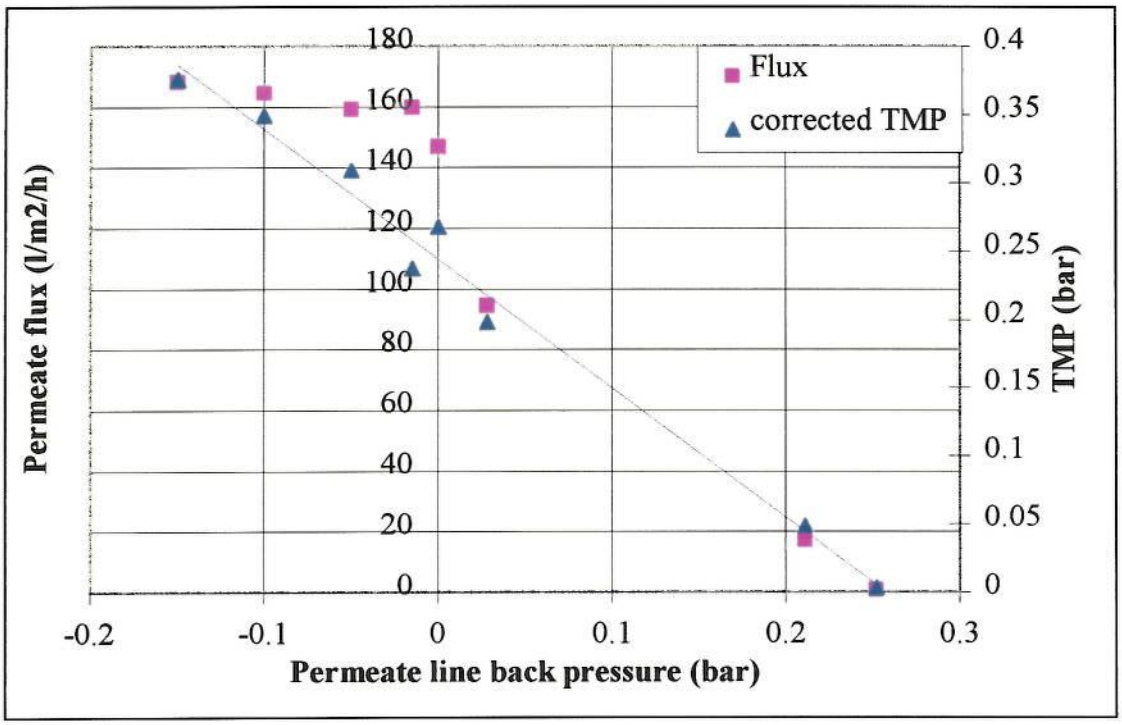

Figure 6.4 Response of permeate flux to changes in ΔP effected with permeate line back pressure

The data points for the permeate flux do not show a good fit to a linear response when the permeate back pressure deviates from atmospheric pressure by a small amount. This does not fit with the theory, and to the authors knowledge, no effect of this nature has been reported.

Further work is required in this area to determine whether this is a real effect or an artefact of the experimental rig used in this study.

6.11.3. Pressure drop through the system:

The frictional losses through the membrane module are high due to the dimensions of the tubular membranes and the cross flow velocities used. As pressure drop is proportional to velocity squared, increasing the cross flow velocity to improve flux will quickly become uneconomical due to the growing losses.

This illustrates the value of using the specific flux to compare the performance of membranes. The value of ΔP (as determined by pressure gauges either side of the membrane module) will include the frictional losses, and therefore gives an accurate guide to the energy used in the filtration.

7. CONCLUSIONS

The results of this study show that there can be significant differences in the performance of membranes that have a similar specification. The variation in the resistance to clean water illustrates this clearly. This is probably due to differences in the pore structure and membrane material.

Allowing for differences between individual membranes, the permeate flux has a strong dependence on the feed solution concentration and cross flow velocity. The permeate flux shows a logarithmic decline with increasing MLSS. In this study, the optimum cross flow velocity in terms of specific flux production is approximately 3 ms^{-1}.

The permeate water quality was consistently high, with SS and BOD_5 normally below the limit of detection. A difference in the levels of DOC between the feed and permeate streams show that the membranes rejected a portion of the high molecular weight molecules in solution.

Pressure drop through the membrane module is dependant on the flow velocity. Consideration should be given to the losses through the system when deciding on an operating regime.

The lowest energy consumption for the filtration was 1.75 $kWhm^{-3}$. This is six times higher than the cost of conventional treatment. The decision to use a side-stream MBR over conventional treatment could be made only if the advantages out weighed the cost penalty. This decision could be driven by:

- Legislation requiring a very high quality effluent
- Land costs prohibiting large scale conventional treatment
- Sludge handling and disposal costs prohibitive
- Specific biological conditions required for high strength wastewater

The MF membrane (M3), with a higher nominal pore size, has produced a higher specific flux in all conditions tested. There is no significant difference in the removal of contaminants, and the tubidity is similar for all membrane types. The increased porosity of the MF membrane benefits the specific flux produced, yet does not compromise permeate quality.

The energy consumption of membrane filtration can be minimised by careful design and trials such as these. The cost of cleaning fouled membranes increases both capital and operating costs. The reduction of these cleaning costs could be achieved if fouling is reduced or limited. Sub-critical flux operation offers this possibility, if the ideal operating conditions can be identified.

8. RECOMMENDATIONS FOR FURTHER WORK

- Two of the membrane modules used in these trials (M1 and M2) have a very similar specification. Their performance under the same conditions shows large differences. The reasons for this must lie with the material and/or pore structure. A thorough investigation of the surface properties of the two materials is recommended. This work would have been completed had samples of both materials been made available to the author by the suppliers.

- The investigation into sub-critical flux operation showed that under the conditions used, a stabilised flux was not produced. Further trials using different conditions and the use of a turbulence promoting device is recommended. The potential cost benefit of sub-critical flux operation warrants time spent conducting further trials. The study should include details of how a turbulence promoter affects operating costs due to the increased pressure drop through the module.

- The high flow rate flushing mode was only subject to preliminary trials during this work. A structured series of experiments varying the periodicity and duration of the flushes is recommended. If a quantifiable effect can be seen, the effect on energy consumption should be assessed in terms of the gain in permeate product.

- Bacteriological analysis of the permeate would be useful to accurately assess the rejection of the membranes. The would be important should the effluent be discharged to a sensitive zone e.g. bathing beaches.

- The flux appears to respond to permeate line back pressure in a non-linear way. The change in gradient of the response appears to occur at around atmospheric pressure. A laboratory scale study would be able to rule out an isolated effect peculiar to the experimental rig used in this study.

9. REFERENCES

Al-Malack, M. H., Anderson, G. K., **Use of microfiltration in wastewater treatment**. *Water Research* **31**(12), 1997, 3064-3072.

American Public Health Asociation (APHA), Standard methods for the examination of water and wastewater. 1989. ISBN 0-87553-161-X

American Water Works Association Research Foundation (AWWARF), Lyonnaise des Eaux (LdE), Water Research Commission (WRC) of South Africa, Water Treatment Membrane Processes. New York: McGraw-Hill, 1996.

Anderson, G. K., James, A. and Saw, C. B., **Crossflow microfiltration - A membrane process for biomass retention in anaerobic digestion.** 4th World filtration congress. Royal Flemish Society of Engineers, 22 - 25 April 1986, Ostende, 11.75 - 11.84.

Arroyo, G., Fonade, C., **Use of intermittent jets to enhance flux in crossflow filtration.** *Journal of Membrane Science* **80**, 1993, 117-129.

Bacchin, P., Aimar, P., Sanchez, V.. **Model for colloidal fouling of membranes.** *AIChE Journal* **41**(2), 1995, 368-376.

Bailey, A. D., Hansford, G. S. and Dold, P. L., **The use of crossflow microfiltration to enhance the performance of an activated sludge reactor.** *Water Research* **28**(2), 1994, 297-301.

Baker, R. J., Fane, A. G., Fell, C.J.D., Yoo, B.H. **Factors affecting flux in crossflow filtration.** *Desalination* **53,** 1985, 81-93.

Beaubien, A., Baty, M., Jeannot, F., Francoeur, E. and Manem, J., **Design and operation of anaerobic membrane bioreactors: development of a filtration testing strategy.** *Journal of Membrane Science* **109,** 1996, 173-184.

Belfort, G. and Altena, F. W., **Toward an inductive understanding of membrane fouling.** *Desalination* **47,** 1983, 105-127.

Belfort, G., **Membrane modules: comparison of different configurations using fluid mechanics.** *Journal of Membrane Science* **35**, 1988, 245-270.

Belfort, G.,. **Fluid mechanics in membrane filtration: recent developments.** *Journal of Membrane Science* **40**, 1989, 123-147.

Bertram, C. D., Hoogland, M. R., Li, H., Odell, R. A., Fane, A. G., **Flux enhancement in crossflow microfiltration using a collapsible-tube pulsation generator.** *Journal of Membrane Science* **84**(3), 1993, 279-292.

Boonthanon, S., Hwan, L. S., Vigneswaran, S., Ben Aim, R., Mora, J. C., **Application of pulsating cleaning technique in crossflow microfiltration.** *Filtration & Separation* **May/June**, 1991, 199-201.

Bowen, W. R., Kingdon, R. S. and Sabuni, H. A. M., **Electrically enhanced separation processes: The basis of in situ intermittent electrolytic membrane cleaning (IIEMC) and in situ electrolytic membrane restoration (IEMR).** *Journal of Membrane Science* **40**, 1989, 219-229.

Brindle, K., Stephenson, T. **The application of membrane biological reactors for the treatment of wastewaters.** *Biotechnology and Bioengineering*, **49**(6), 1995, 601-610.

Choo, K-H. and Lee, C-H.,. **Membrane fouling mechanisms in the membrane coupled anaerobic bioreactor.** *Water Research* **30**(8), 1996, 1771-1780.

Cicek, N., Winnen, H., Suidan, M. T., Wrenn, B. E., Urbain, V. and Manem, J., **Effectiveness of the membrane bioreactor in the biodegradation of high molecular weight compounds.** *Water Research* **32**(5), 1998, 1553-1563.

Cross, S. N. **Membrane fouling and cleaning, a review.** pp.61-90. *Effective industral processes - benefits and opportunities*. Elservier Science, England. 1991.

DeFilippi, R. P., Goldsmith, R. L., **Application and theory of membrane processes for biological and other macromolecular solutions.** *Membrane Science and Technology: Industrial, Biological and Waste Treatment Processes*, Plennum Press, New York, 1970.

Defrise, D. and Gekas, V., **Microfiltration membranes and the problem of microbial adhesion**. *Process Biochemistry* **August**, 1988, 105-116.

Elmaleh, S. and Abdelmoumni, L., **Cross flow filtration of an anaerobic methanogenic suspension.** *Journal of Membrane Science* **131**, 1997, 261-274.

Fakhru'l-Razi, A., **Ultrafiltration membrane separation for an anaerobic wastewater treatment.** *Water Science & Technology* **30**(12), 1994, 321-327.

Fane, A. G., Fell, C. J. D. and Kim, K. J., **The effect of surfactant pre-treatment on the ultrafiltration of proteins.** *Desalination* **53**, 1985, 37-55.

Fane, A. G., Fell, C.J.D. **A review of fouling and fouling control in ultrafiltration.** *Desalination* **62**, 1987, 117-136.

Field, R. W., Wu, D., Howell, J. A., Gupta, B. B., **Critical flux concept for microfiltration fouling.** *Journal of Membrane Science* **100**, 1995, 259-272.

Finnigan, S. M. and Howell, J. A., **The effect of pulsatile flow on ultrafiltration fluxes in a baffled tubular membrane system.** *Chemical Engineering research Des.* **67**(3), 1989, 278-282.

Ghyoot, W., Beeckman, M., Van den Hende, P. and Verstraete, W., **Treatment of low and high strength wastewater with a membrane bioreactor.** International Symposium on Environmental Biotechnology, Part 1, Ostende, 21-23 April, 1997, 94th Event of the European Federation of Biotechnology. Pp67-70.

Green, G. and Belfort, G., **Fouling of ultrafiltration membranes: lateral migration and the particle trajectory model.** *Desalination* **35**, 1980, 129-147.

Gregor, H. P. and Gregor, C. D., **Synthetic membrane technology.** *Scientific American* **239**, 1978, 88-101.

Hanemaaijer, J. H., Robbertson, T., Van Den Boomgaard, Th. And Gunnink, J. W., **Fouling of ultrafiltration membranes. The role of protein adsorption and salt precipitation.** *Journal of Membrane Science* **40,** 1989, 199-217.

HMSO, Ammonia in waters London: HMSO, 1981.

HMSO, Biochemical Oxygen Demand. London: HMSO, 1981.

HMSO, Chemical Oxygen Demand (Dichromate value) of Polluted and waste waters, 2nd edition London: HMSO, 1986.

HMSO, Kjedahl Nitrogen in Waters London: HMSO, 1987.

HMSO, Suspended, Settleable, and Total Dissolved Solids in waters and effluents London: HMSO, 1980.

HMSO, The instrumental determination of Total Organic Carbon, Total Oxygen Demand and related determinands London: HMSO, 1979.

Hodgson, P. H., Fane, A. G., **Crossflow filtration of biomass with inorganic membranes: The influence of membrane surface and fluid dynamics.** *Key Engineering Materials* **61&62,** 1991, 167-174.

Hodgson, P. H., Leslie, G. L., Schneider, R. P., Fane, A. G., Fell, C. J. D., Marshall, K. C., **Cake resistance and solute rejection in bacterial microfiltration: The role of the extracellular matrix.** *Journal of Membrane Science* **79**, 1993, 35-53

Howell, J. A., Finnigan, S. M., **Hydrodynamics and Membrane filtration.** *Effective Industrial membrane processes - Benefits and Opportunities,* 1991, pp.49-60 *Elsevier Science Publishers.*

Howell, J. A., **Sub-critical flux operation of microfiltration**. *Journal of Membrane Science* **107**, 1995, 165-171.

Howell, J., **Membrane processes for the treatment of activated sludge.** Euromembrane 1996, **Part I**: 463-469.

Ishiguro, K., Imai, K. and Sawada, S., **Effects of biological treatment conditions on permeate flux of UF membrane in the membrane/activated sludge wastewater treatment system.** *Desalination* **98,** 1994, 119-126.

Jaffrin, M. Y., Ding, L. H. and Gupta, B. B., **Rationale of filtration enhancement in membrane plasmapheresis by pulsatile blood flow.** *Life Support Systems* **5**, 1987, 267-271.

Koltuniewicz, A., Noworyta, A., **Dynamic properties of ultrafiltration systems in light of the surface renewal theory.** *Ind. Eng. Chem. Res.* **33**, 1994, 1771-1779.

Krauth, Kh. and Staab, K. F., **Pressurised Bio-membrane reactor for wastewater treatment.** *Hydrotop* **94,** 1994, 555-562.

Krauth, Kh. and Staab, K. F., **Pressurised bioreactor with membrane filtration for wastewater treatment.** *Water Research* **27**(3), 1993, 405-411.

Kroner, K. H. and Nissenin, V., **Dynamic filtration of microbial suspensions using an axially rotating filter.** *Journal of Membrane Science*, **36**, 1988, 85-100.

Levy, P. F., Earle, R. S., **The effect of channel height and channel spacers on flux and energy requirements in crossflow filtration**. *Journal of Membrane Science* **91**(1-2), 1994, 135-143.

Magara, Y. and Itoh, M., **The effect of operational factors on solid/liquid separation by ultra-membrane filtration in a biological denitrification system for collected human excreta treatment plants.** *Water Science & Technology* **23**, 1991, 1583-1590.

Metcalf and Eddy Inc. Wastewater engineering: treatment, disposal and reuse. 3rd ed. New York: McGraw-Hill, 1991.

Mikulasek, P., **Methods to reduce concentration polarisation and fouling in membrane filtration.** *Collection of Czechoslovak Chemical Communications* **59**(4), 1994, 737-755.

Muller, E. B., Stouthamer, A. H., van Verseveld, H. W. and Eikelboom, D. H., **Aerobic domestic waste water treatment in a pilot plant with complete sludge retention by crossflow filtration.** *Water Research* **29**(4), 1995, 1179-1189.

Owen, G., bandi, M., Howell, J. A., Churchouse, S. J. **Economic assessment of membrane processes for water and waste water treatment.** *Journal of Membrane Science* **102,** 1995, 77-91.

Perry, R. H., and Green, D. W. (eds) Perry's Chemical Engineers' Handbook, 6th edition New York: McGraw-Hill, 1984.

Persson, K. M., Nilsson, J. L. **Fouling resistance models in MF and UF.** Desalination **80**, 1991, 123-138.

Porter, M. C., Microfiltration. Synthetic Membranes: Science, Engineering and Applications: 225-247. D. Reidel Publishing Company. 1986.

Porter, M.C., **Concentration polarisation with membrane ultrafiltration.** *Industrial Engineering Chemical Products Research and Development* **11**(3), 1972, 234-248.

Rodgers, V. G. J. and Sparks, R. E., **Reduction of membrane fouling in the ultrafiltration of binary protein mixtures.** *AIChE Journal* **37**(10), 1991, 1517-1527.

Sato, T. and Ishii, Y., **Effects of activated sludge properties on water flux of ultrafiltration membrane used for human excrement treatment.** *Water Science & Technology* **23**, 1991, 1601-1608.

Segre, G. and Silbeberg, A., **Behaviour of macroscopic rigid spheres in Poiseuille flow.** *Fluid Mechanics,* **14,** 1962, 115.

Shimizu, Y., Rokudai, M., Tohya, S., Kayawake, E., Yazawa, T., Tanaka, H. and Eguchi, K., **Filtration characteristics of charged alumina membranes for methanogenic waste.** *Journal of Chemical Engineering of Japan* **22**(6), 1989, 635-641.

Smith, C. W., **The use of ultrafiltration membranes for activated sludge separation.** 24th Annual Purdue Industrial Waste Conference, 1969, Purdue University, West Layfette, India. Pp1300-1310.

Suzuki, T., Suwa, Y., Toyohara, H., Yamagishi, T. and Hirai, M., **Effects of organic loading, pH and DO concentration on the dissolved organic carbon removal by an activated sludge process with cross flow filtration.** *Bull. Nat. Res. Inst. & Res.* **18**(1), 1988, 25-29.

Trouve, E., Urbain, V. and Manem, J., **Treatment of municipal wastewater by a membrane bioreactor: results of a semi-industrial pilot-scale study.** *Water Science & Technology* **30**(4), 1994, 151-157.

Ueda, T., Hata, K. and Kikuoka, Y., **Treatment of domestic sewage from rural settlements by a membrane bioreactor.** *Water Science & Technology* **34**(9), 1996, 189-196.

Van Den Berg, G. B. and Smolders, C. A., **Flux decline in ultrafiltration processes.** *Desalination* **77**, 1990, 101-133.

Velicangil, O. and Howell, J. A., **Self cleaning membranes for ultrafiltration.** *Biotechnology and Bioengineering* **23**, 1981, 843-854.

Visvanathan, C., Ben Aim, R. **Studies on colloidal membrane fouling mechanisms in crossflow microfiltration.** *Journal of Membrane Science* **45**, 1989, 3-15.

Wakeman, R. **Fouling in crossflow ultra- and micro-filtration**. *Membrane technology* **70**, 1996, 5-8.

Wang Shu-Sen. **Effect of solution viscosity on ultrafiltration flux**. *Journal of Membrane Science* **39**, 1988, 187-194.

Wang, S. S., Davidson, B., Gillespie, C., Harris, L. R. and Lent, D. S., **Dynamics of enhanced protein ultrafiltration using an immobilised protease.** *Journal of Food Science* **45,** 1980, 700-702.

Winnen, H., Suidan, M. T., Scarpino, P. V., Wrenn, B., Cicek, N., Urbain, V. and Manem, J., **Effectiveness of the membrane bioreactor in the biodegradation of high molecular-weight compounds.** *Water Science & Technology* **34**(9), 1996, 197-203.

Winston Ho, W. S. and Sirkar, K. K., Membrane Handbook. New York: Van Nostrand Reinhold, 1992.

10. APPENDIX A: SPREADSHEET FOR RIG SET-UP

The spreadsheet detailed below was developed to aid set-up and running of the experimental rig.

No. of streams used for concentration process: (1 or 2)	2.00					
Volume of liquor in reservoir m3	800.00		tank cycle	time (min)	reservoir (mg/l)	new conc. (mg/l)
			0.00	0.00	3500.00	
Desired reservoir conc. mg/l	5000.00		1.00	0.80	3517.59	3517.50
			2.00	1.60	3535.26	3535.09
Influent liquor conc. mg/l	3500.00		3.00	2.40	3553.03	3552.76
	Stream 1	Stream 2	4.00	3.20	3570.88	3570.53
			5.00	4.00	3588.83	3588.38
			6.00	4.80	3606.86	3606.33
Flow rate through modules l/min	500	500	7.00	5.60	3624.99	3624.36
			8.00	6.40	3643.20	3642.49
Permeate flow rate l/min	1.5	3.5	9.00	7.20	3661.51	3660.70
			10.00	8.00	3679.91	3679.01
Total Permeate flow rate l/min	5.00		11.00	8.80	3698.40	3697.41
			12.00	9.60	3716.99	3715.90
time taken for 1 res. volume to pass through system (mins)	0.80		13.00	10.40	3735.67	3734.49
			14.00	11.20	3754.44	3753.17
Concentration factor:	1.005		15.00	12.00	3773.30	3771.94
			16.00	12.80	3792.27	3790.80
Flow of new sludge required (assuming all permeate wasted) l/cycle	4.00		17.00	13.60	3811.32	3809.77
			18.00	14.40	3830.47	3828.82
Flow of new sludge required (assuming all permeate wasted) **l/min**	5.00		19.00	15.20	3849.72	3847.97
			20.00	16.00	3869.07	3867.22
			21.00	16.80	3888.51	3886.57

KEY:
REQUIRED VALUE
IMPORTANT SETUP DATA

22.00	17.60	3908.05	3906.01
23.00	18.40	3927.69	3925.55
24.00	19.20	3947.43	3945.19
25.00	20.00	3967.26	3964.93
26.00	20.80	3987.20	3984.76
27.00	21.60	4007.24	4004.70
28.00	22.40	4027.37	4024.74
29.00	23.20	4047.61	4044.87
30.00	24.00	4067.95	4065.11
31.00	24.80	4088.39	4085.45
32.00	25.60	4108.94	4105.89
33.00	26.40	4129.58	4126.44
34.00	27.20	4150.34	4147.08
35.00	28.00	4171.19	4167.84
36.00	28.80	4192.15	4188.69
37.00	29.60	4213.22	4209.65
38.00	30.40	4234.39	4230.72
39.00	31.20	4255.67	4251.89
40.00	32.00	4277.05	4273.17
41.00	32.80	4298.55	4294.55
42.00	33.60	4320.15	4316.05
43.00	34.40	4341.86	4337.65
44.00	35.20	4363.68	4359.36
45.00	36.00	4385.60	4381.18
46.00	36.80	4407.64	4403.10
47.00	37.60	4429.79	4425.14
48.00	38.40	4452.05	4447.29
49.00	39.20	4474.42	4469.55
50.00	40.00	4496.91	4491.92

3.50	1.75	-2.25
4.00	2.00	-2.00
4.50	2.25	-1.75
5.00	2.50	-1.50
5.50	2.75	-1.25
6.00	3.00	-1.00
6.50	3.25	-0.75
7.00	3.50	-0.50
7.50	3.75	-0.25
8.00	4.00	0.00
8.50	4.25	0.25
9.00	4.50	0.50
9.50	4.75	0.75
10.00	5.00	1.00

11. APPENDIX B: SAMPLE ANALYSIS RAW DATA

The raw data from the sample analysis is shown in the tables below.

22-Jun-98	12:30		1490	2470	3.77	13.8	2480	6.3	1700	2470	6.11	17.2	2300	6.6
23-Jun-98	15:00		1730	3060	2.12	15.4	1120	7	1670	3140	2.45	15.4	2680	7.4
mean		PCI & Koch MF	1385	2806.7	5.91	12.3	2456.7	6.3833	1563.3	2956.7	5.718	12.15	2496	7.15
SD			253.6	255.16	3.3303	4.9493	758.36	0.9042	324.2	401.83	4.067	6.3551	207.1	0.653
30-Jun-98	12:00		1200	2180	3.74	12.7	2160	6.6	1740	2950	18.3	50	3600	34.6
01-Jul-98	13:00		1210	3370	10.1	110	1800	41.6	1419	3090	8.01	174	2410	123
02-Jul-98	15:30	5,000 mg/l,	2000	4230	45.5	231	3690	30.2	2040	4830	9.62	257	4870	16
05-Jul-98	12:00	aerobic recycle	1250	3500	3.32	201	3070	35	1410	3550	16	206	4080	48.8
06-Jul-98	13:00		1390	3310	0.41	202	3070	8	2060	5010	4.77	314	4720	10
mean		PCI & Koch MF												
SD														
06-Jul-98	17:00		1980	4730	2.4	272	4550	7.5	2020	5120	5.78	324	4520	9.6
08-Jul-98	12:00		1450	3870	5.62	10.4	2590	7.5	2190	3890	9.68	53.7	4790	13.4
09-Jul-98	15:00		1710	3370	1.26	17.5	2820	8.2	2670	6260	5.08	88.1	4920	12.3
14-Jul-98	13:30		900	3340	1.84	247	3410	8.9	900	4220	4.36	260	4850	9.8
mean		PCI & Koch UF	1526	3764.3	8.6214	168.7	3314.3	15.043	1898.6	4697.1	7.899	214.69	4679	17.13
SD			399.4	543.5	16.348	108.59	653.91	12.083	573.98	906.64	4.213	106.2	294.9	14.16
16-Jul-98	12:30	commutated PCI on st2	2245	1100	2.01	82.4	2240	8.5	2466	923	9.25	104	4520	16.5
17-Jul-98	15:30		1530	1450	9.02	10.6	2850	10.8	1450	412	5.8	17.5	2680	20.9
20-Jul-98	15:15		2259	5780	0.108	65.9	8090	15.9	2226	6450	0.173	17.9	7530	16.2
22-Jul-98	12:30	15,000 mg/l settled sludge UF	2800	8500	0.55	60.6	7720	14.3	3166	16200	24.6	162	15500	10.8

23-Jul-98	15:30		3250	5190	8.66	47.2	5950	10.6	2750	14910	17.4	181	14200	18.7
mean		PCI & Koch MF	3025	6845	4.605	53.9	6835	12.45	2958	15555	21	171.5	14850	14.75
SD			318.2	2340.5	5.7346	9.4752	1251.6	2.6163	294.16	912.17	5.091	13.435	919.2	5.586
25-Jul-98	14:00		2760	6240	38.2	127	6290	50.3	3125	7810	58.1	85	6920	89.2
27-Jul-98	10:35		1730	1990	3.62	31.1	2720	9.81	1820	2360	4.57	41	2940	8.44
28-Jul-98	16:00		2340	2940	5.39	22.5	2980	11.9	2660	2740	5.78	23.5	2960	10.3
30-Jul-98	16:00		1570	2360	1.4	25.5	3370	8.17		4990	4.97	37.7	5300	10.6

Date	time	Run type	Permeate stream 1						Permeate stream 2					
			BOD	COD	NH3-N	TKN	SS	DOC	BOD	COD	NH3-N	TKN	SS	DOC
04-Jun-98	15:00	7,500 mg/l,	2	16	0.08	6.4	2	5.9	2	15.1	0.03	1.4	2	5.2
08-Jun-98	15:00	settled sludge	2	18.8	0.03	1.5	2	5.9	2	18.2	0.07	1.2	2	5.2
09-Jun-98	15:00		2	28.1	0.86	5.7	2	8.2	2	20.6	0.49	1.3	2	6
mean		PCI &Koch UF							2	17.96667	0.196667	1.3	2	5.466667
SD									0	2.757414	0.25482	0.1	0	0.46188
10-Jun-98	15:00		2	33.6	0.65	2.6	2	7	2	28	0.83	2	2	6.3
11-Jun-98	15:00		2	14.9	0.23	3.5	2	7	2	43.7	0.91	2.2	3.2	7.6
13-Jun-98	15:00		2	21.6	1.4	1	2.67	5.9	2	17.8	1.49	1.8	10.4	4
mean		PCI &Koch MF	2	22.167	0.5417	3.45	2.1117	6.65	2	29.83333	1.076667	2	5.2	5.966667

06-Jul-98	13:00		2	38.8	3.63	2.1	2	7.1	2	22	3.8	3.4	2	6.3
mean		PCI & Koch MF							2	20.866 67	2.86	2.666 667	2	6.666 667
SD									0	1.0016 65	0.81504 6	0.635 085	0	0.472 582
06-Jul-98	17:00		4.19	20.6	5.03	6.2	2	11.1	2	18.9	4.82	4.5	2	5.8
08-Jul-98	12:00		2	28.1	3.72	4.2	2	8.4	2	21.5	3.72	3	2	6.4
09-Jul-98	15:00		2.11	32.9	3.77	5.3	5	8.8	2	15.2	3.71	4.9	4.5	8
14-Jul-98	13:30		2	26	1.86	3.9	3.2	10.2	2	15	2.11	1.9	2	6.7
mean		PCI & Koch UF	2.3286	26.771	3.2171	3.5857	2.6	8.3143	2	17.65	3.59	3.575	2.625	6.725
SD			0.8218	7.1547	1.1337	1.8096	1.1489	1.881	0	3.1310 28	1.11573 6	1.384 136	1.25	0.928 709
16-Jul-98	12:30	commutated PCI on st2	2	18.8	2.78	7.9	2	9.1	2	19.1	2.8	9.3	2	8.4
17-Jul-98	15:30		2	21.2	0.03	2.1	2	5.7	2	36.8	0.07	1.5	2	7.5
20-Jul-98	15:15		2	16.9	1	1.2	2.5	5.6	2	20.2	1.31	1	2	7.5
22-Jul-98	12:30	15,000 mg/l settled sludge UF	2.85	34.7	7.35	9.1	2.8	9.1	4.62	54.7	7.24	6.1	2.4	12.2
23-Jul-98	15:30		6.79	39.9	5.61	5.2	8	11.7	2.14	26.1	5.66	1	2	8.9
mean		PCI & Koch MF	4.82	37.3	6.48	7.15	5.4	10.4						
SD			2.786	3.677	1.2304	2.7577	3.677	1.8385						
25-Jul-98	14:00		3.48	42.9	9.74	14.1	17	11.5	2	38	9.93	9.61	6.7	10.4
27-Jul-98	10:35		3.14	21.6	0.03	1	6.7	6.99	2	19.9	0.11	1	5.5	6.94
28-Jul-98	16:00		10.1	18.8	0.3	1.1	7.8	8.02	13	17.3	0.85	1.6	2	7.91
30-Jul-98	16:00			27.5	4.42	1	2	7.6	2	22.5	4.14		2	7.54

12. APPENDIX C HEADLOSS CALCULATION DETAILS

Where the feed flow enters the module, it is subject to a change in cross sectional area. This change in area can be calculated knowing the diameter of the feed pipe and that of each membrane tube:

Cross sectional area of feed pipe = $\pi * (0.075)^2$ =

$0.018\ m^2$

Total cross sectional area of membrane = $\pi * (0.012)^2 * 19$ =

$0.0086\ m^2$

Therefore reduction in cross sectional area = 0.018/0.0086 =

2.1:1

The k values are shown in the table below:

Fitting	**loss coefficient, k**
90^0 close radius bend	0.75
90^0 long radius bend	0.4
Sudden enlargement, 1:5	1.0
Sudden reduction in cross sectional area, 2:1	0.4